

# WP2 – Deliverable 2.4

## Report on Seismic Reprocessing, West Macedonia

Release Status: Public

Authors: Dimitrios Ktenas, George Makrodimitras, Konstantinos Tzimeas,  
Efthimios Tartaras (Hellenic Hydrocarbons and Energy Resources Management  
Company - HEREMA)

Edited by Mark Wilkinson

Date: 13th December 2024

Filename and Version:

PilotSTRATEGY\_WP2\_D2.4\_SeismicInterpReport\_MHB\_Final

Project ID Number: 101022664

PilotSTRATEGY (H2020- Topic LC-SC3-NZE-6-2020 - RIA)

## 1. Document History

### 1.1 Location

This document is stored in the following location:

<b>Filename</b>	PilotSTRATEGY_WP2_D2.4_SeismicInterpReport_MHB_Final.pdf
<b>Location</b>	

### 1.2 Revision History

This document has been through the following revisions:

Version No.	Revision Date	Filename/Location stored:	Brief Summary of Changes
V.1	29 Nov 2024	PilotSTRATEGY_WP2_D 2.4_SeismicInterpReport_MHB_Vol1	1 <sup>st</sup> Draft
V.2	6 <sup>th</sup> Dec 2024	PilotSTRATEGY_WP2_D 2.4_SeismicInterpReport_MHB_Vol2	2 <sup>nd</sup> Draft
V.3	13 <sup>th</sup> Dec 2024	PilotSTRATEGY_WP2_D 2.4_SeismicInterpReport_MHB_Final	Final version reviewed by coordinator

### 1.3 Authorisation

This document requires the following approvals:

AUTHORISATION	Name	Signature	Date
WP Leader	Mark Wilkinson	MW	13/12/2024
Project Coordinator	Isaline Gravaud	IG	13/12/2024

### 1.4 Distribution

This document has been distributed to:

Name	Title	Version Issued	Date of Issue
		Public	18/12/2024

© European Union, 2024

No third-party textual or artistic material is included in the publication without the copyright holder's prior consent to further dissemination by other third parties.

Reproduction is authorised provided the source is acknowledged.

Ktenas D., Makrodimitras G., Tzimeas K., Tartaras E., 2024. Report on Seismic Reprocessing, West Macedonia. Deliverable D2.4. EU H2020 PilotSTRATEGY project 101022664, report, pp44.

### **Disclaimer**

The information and views set out in this report are those of the author(s) and do not necessarily reflect the official opinion of the European Union. Neither the European Union institutions and bodies nor any person acting on their behalf may be held responsible for the use which may be made of the information contained therein.



## 2. Executive summary

The Mesohellenic Basin (MHB) seismic interpretation study, conducted as part of the Horizon 2020-funded PilotSTRATEGY project, aims to enhance the assessment of the CO<sub>2</sub> storage resource in the area. This work aimed to advance these resources toward contingent status based on available legacy seismic data. Situated in Western Macedonia, onshore Northern Greece, the MHB represents a prominent sedimentary basin within the Tethyan orogenic belt, which is characterised by complex tectonic evolution and sedimentary processes.

The report provides an overview of the basin's geological framework, outlining its geodynamic evolution and stratigraphy. The MHB developed as a piggy-back basin, with stratigraphic formations that include potential reservoir units including the Eptachorion and Pentalophos formations. These units are characterised by turbiditic deposits and significant lithological variations due to tectonic and sedimentary dynamics.

Well data from Neapolis-1 and Neapolis-2 wells confirmed deepwater turbiditic environments and identified seal units suitable for CO<sub>2</sub> storage. Reprocessed seismic data gave enhanced subsurface imaging, revealing eight key horizons and sequences (e.g. Tsotyli and Pentalophos formations). The study identified structural and stratigraphic traps, such as anticline and fault-related features, highlighting the basin's resource potential.

The study's findings significantly advance the geological understanding of the MHB, particularly its suitability for CO<sub>2</sub> storage. The identification of key structural and stratigraphic features, combined with improved seismic imaging, positions the basin as a promising candidate for CO<sub>2</sub> storage projects. However, further research and data collection are crucial to fully unlock its potential and address existing uncertainties.

## Table of Contents

<b>1. Document History</b> .....	<b>1</b>
<b>1.1 Location</b> .....	<b>1</b>
<b>1.2 Revision History</b> .....	<b>1</b>
<b>1.3 Authorisation</b> .....	<b>1</b>
<b>1.4 Distribution</b> .....	<b>1</b>
<b>2. Executive summary</b> .....	<b>3</b>
<b>3. Geodynamic evolution</b> .....	<b>5</b>
<b>3.1. Overview</b> .....	<b>5</b>
<b>4. Stratigraphy</b> .....	<b>7</b>
<b>4.1 Rizoma and Krania Formations</b> .....	<b>8</b>
<b>4.2 Eptachorion Formation</b> .....	<b>10</b>
<b>4.3 Taliaros and Pentalofos Formations</b> .....	<b>11</b>
<b>4.4 Tsotyli Formation</b> .....	<b>12</b>
<b>4.5 Ondria and Orlia Formations</b> .....	<b>12</b>
<b>5. Well data</b> .....	<b>13</b>
<b>5.1 Neapolis-1</b> .....	<b>14</b>
<b>5.2 Neapolis-2</b> .....	<b>16</b>
<b>6. Legacy Seismic data and interpretation</b> .....	<b>19</b>
<b>6.1 Geophysical research and available data</b> .....	<b>19</b>
<b>6.2 Interpreted horizons</b> .....	<b>23</b>
<b>6.3 Seismic sequence and facies</b> .....	<b>24</b>
<b>6.4 Regional seismic interpretation</b> .....	<b>27</b>
<b>6.5 Regional Mapping &amp; traps</b> .....	<b>32</b>
<b>7. Conclusions</b> .....	<b>38</b>
<b>8. References</b> .....	<b>39</b>

### 3. Geodynamic evolution

#### 3.1. Overview

The Mesohellenic Basin (MHB) (or Mesohellenic Trough) in the middle of continental Greece (**Fig.1**) is a major sedimentary basin of the Tethyan orogenic belt. This basin extends from Albania to northern Greece, at the boundary between the two main structural zones of the Hellenides: to the east, the internal zones, that were submitted to obduction in the Jurassic, and, to the west, the external zones which were only tectonized during the Cenozoic (Ferrière et al., 2013).

The underlying basement rocks of the MHB include limestones and ophiolites that formed in an early Mesozoic small ocean basin (Pindos basin). Ophiolites were emplaced eastward onto the Pelagonian continental margin in the middle Jurassic (Robertson, 1996) and the Pindos basin experienced Cretaceous to Eocene compression due to the convergence of the Apulian continental margin with the Pelagonian microcontinent (Fig.1), with supracrustal rocks thrust westward over the Apulian foreland (Doutsos et al., 1993, Kontopoulos et al., 1999).

There is a debate in the academic community regarding the origin of the MHB, which would be either a retro-arc foreland basin (Doutsos 1994); a strike-slip half graben (Zelilidis et al., 2002); a large piggy-back basin (Ferrière et al., 2004); or mostly a pull-apart basin (Vamvaka et al., 2006). The MHB is located near the basement suture between the Pelagonian and Apulian continental blocks. It developed from the late Eocene as a piggy-back basin along the eastern flanks of a giant pop-up structure bounded by the Eptachori thrust, an east-verging back thrust (Doutsos et al., 1994). The Mesohellenic basin shows a tectonically controlled variation in basin evolution along its axis (Doutsos et al., 1994; Zelilidis & Kontopoulos, 1997; Zelilidis et al., 1997). The presence of two small indentors at the southern and northern terminations of the basin induced a tectonic escape towards the central part of the basin until the middle Miocene. Sedimentation along the length of the basin was relatively uniform during the early Oligocene but became more variable during the late Oligocene-early Miocene and was accompanied by different subsidence (Zelilidis, 1997, Kontopoulos et al., 1999).

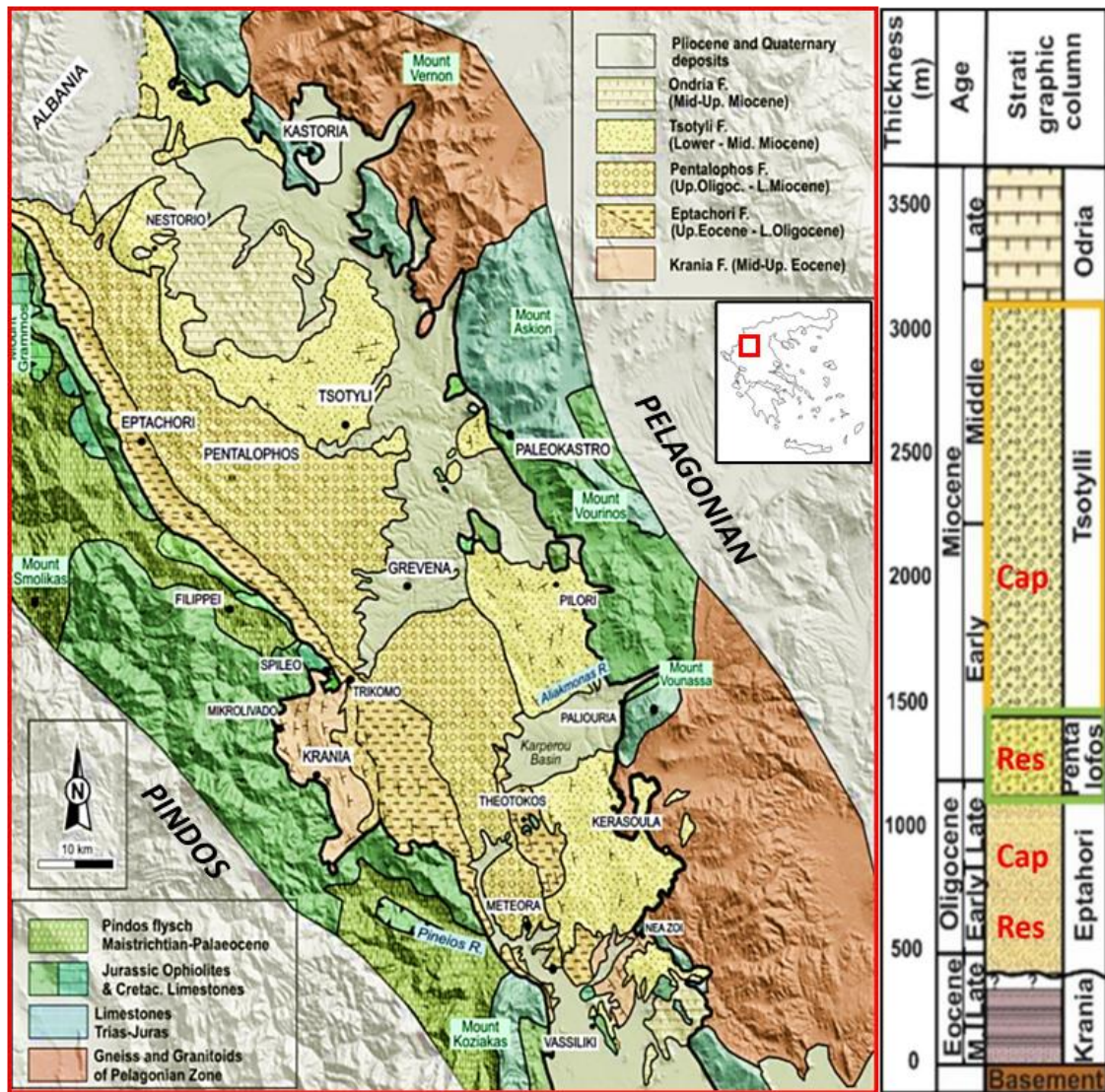
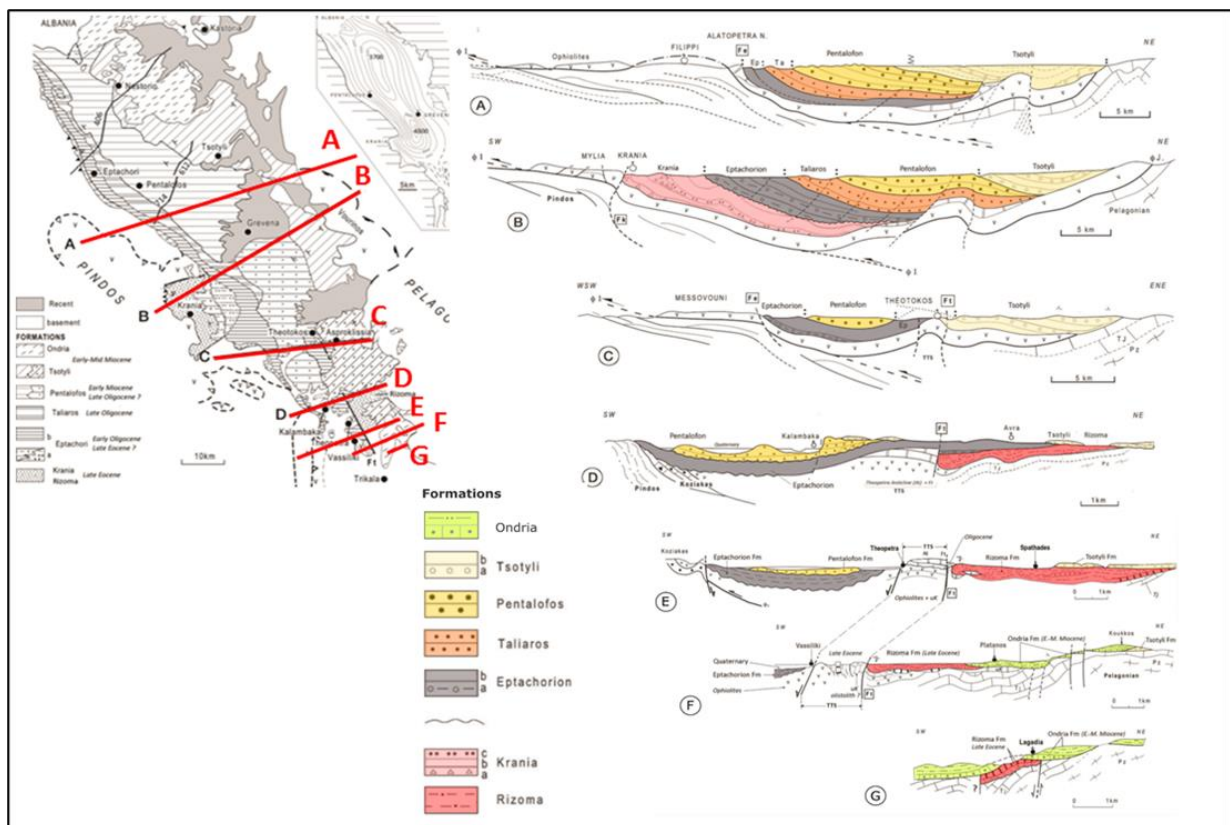


Fig.1. Geological map with ground surface facies distribution in the Mesohellenic Basin, modified after Koukouzas et al. (2018). The study area location is indicated in the inset map.

## 4. Stratigraphy

The large thickness of the MHB strata, the repetitive stacking of gravity deposits (e.g. turbidites) and uncertainties about their lateral and vertical correlation across the basin bring about uncertainties on the definition of large-scale lithological units of stratigraphic significance (Fig.2). Moreover, the chronostratigraphy of MHB Formations is still not very precisely known, mostly because of the scarcity of fossils or due to their reworking in gravity dominated facies (Ferrière et al., 2013).

The only available ages are from marls which include pelagic foraminifera (fossils) or from a few carbonate shelf intervals which include benthic foraminifera and other invertebrates. Moreover, published ages are significantly variable, even for the same faunal associations as nanofossils (Zygojiannis and Müller, 1982; Kontopoulos et al., 1999; Zeligidis et al., 2002; Ferrière et al., 2004). The thickest, deepest and more extended Oligo-Miocene marine formations crop out in the northern part of the MHB basin. Middle-upper Eocene deposits are exposed in restricted area of the centre of the basin (near Krania village). These formations have their chronostratigraphical equivalents to the south of the basin, but there the facies here point to shallower water depths (excluding the Pentalofon Formation in the Meteora area) and therefore hiatuses and gaps in the stratigraphy are frequent (Ferrière et al., 2013).



**Fig.2.** Outcropped formations in the MHB. Modified after Ferrière et al. (2013), Zeligidis et al. (2002) and Kontopoulos et al. (1999).

The Oligocene to Miocene siliciclastic deposits were first described as six main lithostratigraphic units (**Figs 2 and 3**) by Brunn (1956, 1960) from the northern part of the MHB with the addition of a late Eocene Formations (Rizoma Fm and Krania Fm). These Formations are (oldest first):



- i) Rizoma and Krania Formations (about 1500m) dominated by shales with massive sandstone interbeds, locally overlying conglomerates and limestones hosting a benthic macrofossil fauna (Savoyat et al., 1969; Zygojiannis and Muller, 1982).
- ii) Eptachorion Formation (about 1000m, mainly Oligocene) dominated by silty marls in the upper part of the Formation with decimetric thick very fine sandstone beds often resting on thick conglomerates in the lower part.
- iii) Taliaros (or Tsarnos) and (iv) Pentalophos Formations (2500m, latest Oligocene and early Miocene): sandstone beds coarsening upwards to conglomeratic beds; mainly conglomeratic beds in the south (Ori and Roveri, 1987; Ferrière et al., 2013).
- v) Tsotyli Formation ((600m, early-mid Miocene (?)): marls interbedded with sandstones in the northern MHB; gneissic pebbles rich conglomeratic beds in the south (Savoyat et al., 1971a; 1971b; 1972a; 1972b; Zygojiannis and Muller, 1982; Ferrière et al., 2004).
- vi) Ondria and Orlias Formations (350m or more, early-mid Miocene): sandstones and marls with fossiliferous limestone beds.

The formation boundaries are either major angular unconformities or/and abrupt changes in lithology. Angular unconformities record periods of major tectonic deformation. Amongst those, one may cite, in chronological order, the lower boundaries of: the Krania and Rizoma formations (Upper Eocene); the Eptachorion Formation (Oligocene); and the Tsotyli Formation (Miocene). In the southern part of the MHB, the lower Tsotyli bounding unconformity reflects a major change in depocenter location, shifting to the Rizoma area, where Miocene deposits rest above Upper Eocene, Mesozoic or Paleozoic strata (Zelilidis et al., 2002; Ferrière et al., 2013).

## 4.1 Rizoma and Krania Formations

**Rizoma Formation (Fig.3)** rests unconformably above the Pelagonian basement, crops out to the SE of the MHB only and it is covered by Oligocene basal conglomerates or Miocene conglomeratic Tsotyli beds. The Rizoma Formation is dominated by shales with massive sandstone interbeds, locally overlying conglomerates and limestones hosting a benthic macrofossil fauna (Savoyat et al., 1969; Zygojiannis and Muller, 1982). The shales and sandstones have been interpreted as a fluvial-dominated shelf delta system (Ferriere et al., 1998; 2004).

The Rizoma Formation comprises three lithological units, from base to top:

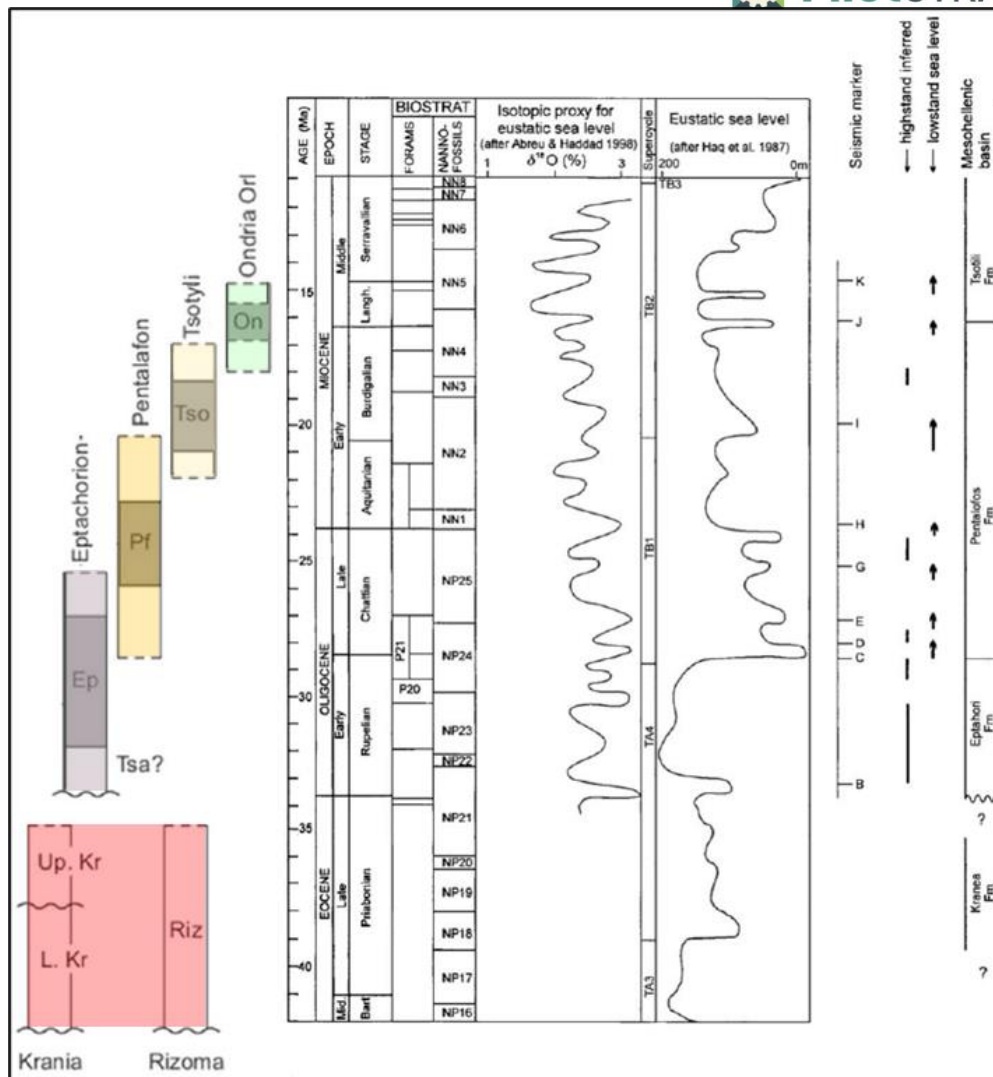
- i) Well-rounded **basal conglomerates**, they include numerous clasts of Cretaceous limestone, as well as radiolarites, ophiolites and Triassic-Jurassic marbles, all derived from the internal zones which crop out in the vicinity to the east.
- ii) **Nummulitic-rich limestones**, pointing to a carbonate shelf setting. They also contain algae and Echinoids and are attributed to the Upper Lutetian (Middle Eocene; Savoyat et al., 1969; 1972a; Ferriere 1982).
- iii) The **“Rizoma marls”**, a thick shale succession (more than 200m) made up of distal turbiditic sequences, locally with m-scale sandstone beds interpreted as fluvial dominated deltaic mouth bar systems with wood fragments; floating mud pebbles; water escape features; current ripples, *Skolithos* and other burrows. This deposit was eroded from the pre-ophiolitic basement of schists and gneisses. Globigerinids.

- iv) (foraminifera: Savoyat et al., 1969; 1972a) and calcareous nannofossils (Zygojiannis and Muller, 1982; Ferrière et al., 2004) from the Rizoma calcareous marls have yielded an Upper Eocene age.

**The Krania Fm (Fig.3)** is thick, laterally continuous and preserved only inside a syn-sedimentary syncline. This formation is exposed in the western part of the MHB, to the SW of Grevena. It forms a **flysch-like unit** 1500 m thick, bounded at the base by ophiolitic conglomerates and mostly overlying the ophiolitic basement of the basin. It is bounded to the top by the major intrabasinal unconformity of the MHB. A minor unconformity has been identified within the formation, separating the Lower and Upper Kranea sequences (Koumantakis and Matarangas, 1980; Wilson, 1993; Ferrière et al., 2004). The Krania Fm contains a foraminifera and nannofossil assemblage dating to the upper Lutetian-Upper Eocene. The Krania Formation exhibits a set of two sequences of deposits:

**Lower Kranea sequence:** West of Krania, the deposits overlie roughly bedded, polygenic clast-supported conglomerate beds, which are interpreted as alluvial fan-delta deposits, onlapping a basement of ophiolitic epiclastites. Above these basal beds, in the Krania-Microlivadon areas, the lower sequence is composed of fine-grained fining upwards and homogeneous sandstone beds interpreted as deep water and ophiolitic rich turbidite.

**Upper Kranea sequence:** This unit unconformably rests above the lower sequence. The unconformity is well exposed on the northern side of the Krania syncline (Triкомо-Monachiti area), while it is less prominent southward, in the center of the syncline. The upper Kranea sequence is made up of similar turbiditic sandstones as the lower one but at the base a sharp-based hectometric succession of thicker beds with locally abundant burrows (*Skolithos*); plant fragments; water escape structures and intraclastic breccias, which are interpreted as part of a basin floor fan.



**Fig.3.** Eustatic sea level variations compared to the MHB lithologic formations ages showing the uncertainties concerning the eustatic control of the MHB evolution (Kr: Krania; Riz: Rizoma; Tsa: Tsarnos; Ep: Eptachori; Pf: Pentalofos; Tso: Tsoyli; On: Ondria; Ori: Orlia Fm). Right part of Fig.3 from Zelilidis et al. (2002); left part from Ferrière et al. (2013).

## 4.2 Eptachorion Formation

**The Eptachorion Fm (Fig.3)** is ubiquitous throughout the MHB. It forms the lower part of the main Oligo-Miocene, NW-SE trending “Albano-Thessalian” basin. It is exposed mostly in the western border of the basin, while it is buried beneath Miocene formations to the east. To the south, the Theotokos-Theopetra anticline (TTS) allows part of this formation to be exposed in the center of the MHB.

The facies are mostly marine siliciclastics but limestones are locally present at the base of the formation. The age of the formation based on dating of benthic foraminifera (at its base), and calcareous nannofossils and planktic foraminifera (at the top), is determined to be Oligocene.

### Facies of Base

The PilotSTRATEGY project has received funding from the European Union’s Horizon 2020 research and innovation programme under grant agreement No. 101022664



@PilotSTRATEGY  
www.pilotstrategy.eu  
Page 10

**Limestones:** Where the Oligocene transgression comes onto hard substrates, namely Mesozoic limestones, shallow-water carbonate reefs develop, and they might there replace the basal conglomerates of the Eptachorion formation. These facies are in turn rapidly buried by fine-grained turbidites.

**Conglomerates:** They record the major tectonic phase of the Eocene/Oligocene boundary. These conglomerates may reach 1,5 km in thickness. The clast lithology of these conglomerates reflects the bedrock lithology of the basement highs exposed in the vicinity of the outcrops. To the west of the basin, they consist of mostly ophiolitic clasts derived from the Pindos area, while to the east the clasts are mostly composed of gneisses derived from the Pelagonian zone.

### 4.3 Taliaros and Pentalofos Formations

#### **Lower part - Taliaros Fm.**

This formation does not exist to the south of the MHB. It is composed of sandstones, marls and gravelly limestones rich in scaphopods and ahermatypical (non-reef-building) corals (Brunn, Pentalofon map, 1960). The sandstones are well bedded (to the north of Alatopetra for instance). They are interpreted as submarine inner and outer fan deposits (Kontopoulos et al., 1999) or distal to proximal turbidites based on their sandstone-shale ratio (Zelilidis et al., 2002). Near Eptachorion village, mass-wasting features are preserved in these facies (slumps).

#### **Main part - Pentalofos Fm**

**The Pentalofos Fm (Fig. 3)** is attributed to the upper Oligocene to lower Miocene. The deposits are mainly coarse-grained detrital sediments (sandstones and conglomerates), deposited in deeper water in the northern part of the MHB than in its southern area. The marine conglomerates and sandstones record an increase in energy of sedimentary processes compared to the Oligocene sediments. This is the response to the uplift of the eastern border of the MHB. One major characteristic of this formation is a sediment source fully located in the internal zones (Pelagonian basement) to the east of the basin, which supplied mostly Paleozoic gneisses and Triassic marbles (Brunn, 1956). This eastern feeder was already active in the Oligocene but subordinate to the Pindos zone (to the west), which was then probably higher and composed of more weatherable and erodible material (ophiolites and flysch).

The mainly marine deposits of the Pentalofos Fm, range from well bedded conglomerates (“Lower Meteora Conglomerats” – LMC) to marly shales. These facies commonly form thickening and coarsening upward successions, first interpreted as shelf deltas (Desprairies, 1979) and later re-interpreted as deep-sea fan turbidites. In its southeastern part of the area the Pentalofos Formation is coarser grained and has been interpreted as fan- and shelf deltas, including the famous Gilbert deltas of the Meteora area (Ori and Roveri, 1987) which fill the MHB and give rise to a regressive event.

## 4.4 Tsotyli Formation

**The Tsotyli Formation (Fig. 3)** is heterogeneous, ranging from continental, coarse-grained deposits to the south, to fine-grained marine facies to the north, of late Aquitanian-Burdigalian (Miocene). To the south, in the Meteora area, it consists mostly of very coarse conglomerates alternating with poorly bedded sandstones mapped as the “Upper Meteora Conglomerates” (Savoyat et al., Kalabaka sheet 1972a). There, the relative amount of clasts derived from the older Pelagonian basement (mostly pre-Triassic gneisses) increases as compared to the underlying Pentalofon Formation.

These various facies are gathered into a unique formation defined as: (i) a separate, distinct depocenter on the eastern side of the MHB; (ii) a set of deposits bounded at the base by the same, major unconformity which is well expressed in the Meteora area (angular unconformity of about 20° between the Lower and the Upper Meteora Conglomerates). This depocenter has the shape of a syncline parallel to the strike of the MHB. The Tsotyli strata inside this syncline show an eastward offlap, which indicates the progressive eastward displacement of accommodation and, therefore, subsidence. To the south of the MHB, the western side of this syncline is an old structural high, the “Theopetra-Theotokos Structure” (TTS). On the eastern flank of the syncline, the upper units of the UMC are overlying Rizoma Eocene deposits or the basement of the MHB.

## 4.5 Ondria and Orlia Formations

The youngest deposits are preserved as two distinct formations at the two ends of the basin. The **Ondria Formation, (Fig.3)**, is composed of alternating sandstones, limestones and marls, while the uppermost **Orlia Formation**, which cover a more restricted area, is composed of sandstones and bioclastic carbonates. To the south of the MHB, only the time equivalent of the Ondria Fm is exposed.

### Ondria Formation

The Ondria Fm is of Burdigalian age (Miocene) and comprises several formations of higher order based on lithology:

- the **Omorfoklissia Formation** (sands and sandstones with interbedded Globigerinid-rich marls);
- and **Zevgostation Formation** (also alternating sands and sandstones with marly intervals).

### Orlia Formation

This formation occupies a restricted area. Upper Miocene age and comprises sandy marls, sandstones and bioclastic carbonates, mostly composed of green algae, echinoids and molluscs (*Ostrea* cf *Crassissima notamment*). Owing to the fact that they were emplaced in very shallow water depths (photopicgreen algae), these deposits might correspond to the final infilling of the last marine area within the MHB (Ferrière et al., 2013).

## 5. Well data

In 1967 two appraisal boreholes, **Neapolis 1 (NP-1)** and **Neapolis 2 (NP-2)**, were drilled in the wider area of the local community of Neapolis, of the regional community of Kozani, Greece (**Fig.4 and Table 1**). A logging survey has been carried out on both of the boreholes. Both wells penetrated the series of marls and sandstone of the Tsotyli Formation without meeting the target reservoir structure.

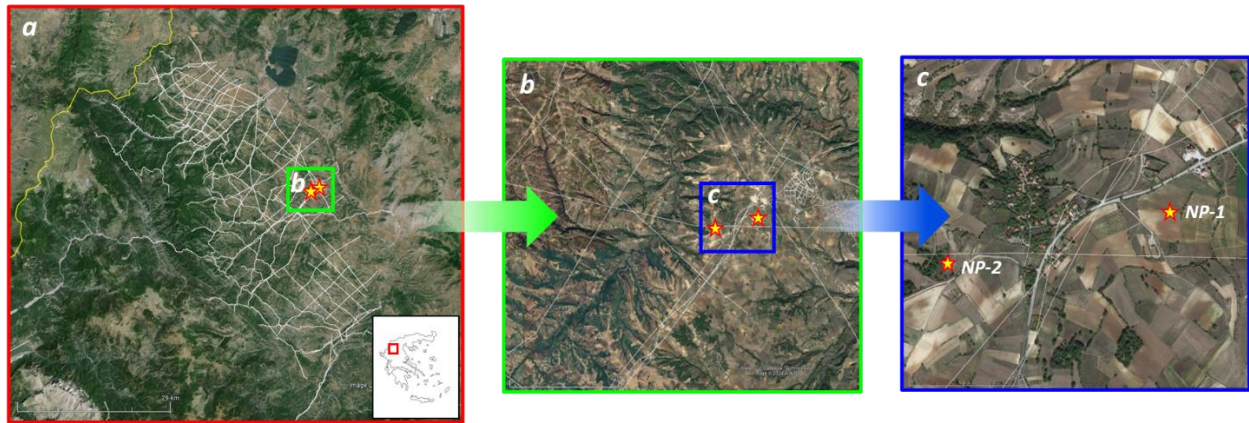


Fig.4. Location maps of Neapolis-1 and Neapolis-2 wells in MHB

**Table 1. Neapolis-1 and Neapolis-2 wells**

Well		Neapoli-1	Neapoli-2
WGS84	Longitude	21°21'56.71"E	21°21'18.71"E
	Latitude	40°18'42.67"N	40°18'35.78"N
Elevation (m)		713.0	720.0
Distance (m)		922.0	
Drilling Depth (m)		691.0	1126.4
Available .las files		Gamma Ray (GR), Neutron Porosity (NEU), Sonic (DT), Electrical, Spontaneous Potential (SP), Volatile hydrocarbon (S1)	Gamma Ray (GR), Sonic (DT), Electrical, Spontaneous Potential (SP), Volatile hydrocarbon (S1), (NNTS), Integrated Sonic Transit Time (ITT), Calcimetry

## Neapolis-1

### Well synopsis

According to National Hydrocarbon Archive reports (Alexiadis, 1995), the Neapolis-1 well was drilled in the eastern flanks of the MHB (**Table 2 and Fig.4**), and penetrated the Tsotyli Formation series, of age Aquitanian-Burdigalian, and reached the Cretaceous carbonate basement (**Fig.5**).

At this location, the Tsotyli Fm is dominated by alternations of mudstone/marls and argillaceous sandstones, with minor siltstone, breccia and conglomerate deposits. From 0-600m the Tsotyli Fm sediments are grey marls, silty sandstone and sandy conglomerates. The interval from 600-609m is brecciated basement rock, a Cretaceous rudist limestone which extends from 609m to the bottom of the borehole. The bedrock and the transition zone between Tsotyli Formation and bedrock has three (3) available cores, all fully recovered (**Fig.5, See Appendix**).

**Table 2. Neapolis-1 well details**

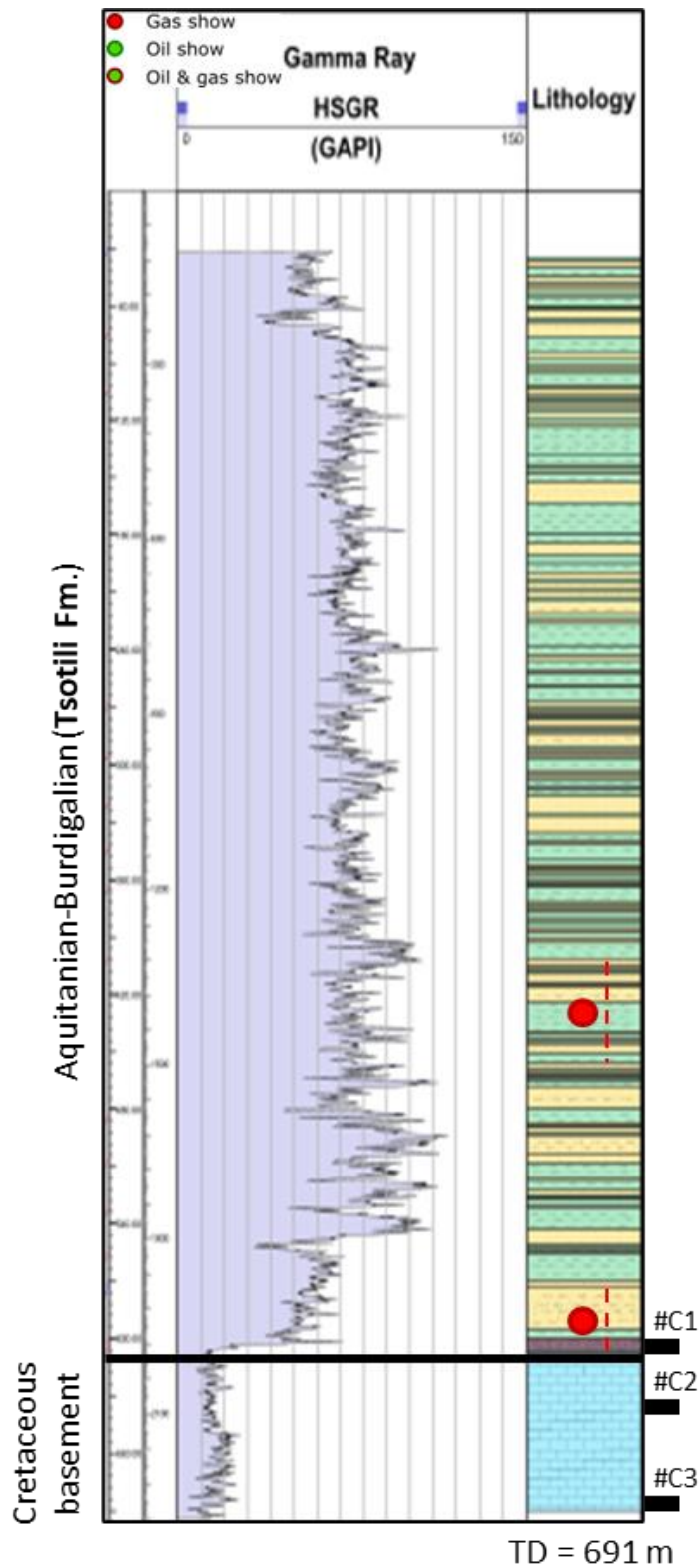
<b>Basin</b>	Mesohellenic (MHB)
<b>Longitude</b>	21°21'56.71"E
<b>Latitude</b>	40°18'42.67"N
<b>Shows</b>	Gas shows (methane)
<b>Elevation</b>	713.00 m
<b>Operator</b>	IFP
<b>Spud</b>	20.12.1966 - 01.01.1967
<b>Total Depth (TD)</b>	691.00 m
<b>Available .las files</b>	Gamma Ray (GR), Neutron Porosity (NEU), Sonic (DT), Electrical Resistivity 16', 18' and 64', Spontaneous Potential (SP), Volatile hydrocarbon (S1)
<b>Geochemical information</b>	400-460m: traces-0.005% methane 580-600m: traces-0.005% methane

### Facies Associations analysis results

A hierarchical approach to sedimentological description and interpretation has been applied to generate lithotypes through cuttings and core data, which were later grouped into depositional packages with similar characteristics and internal organization. The vertical and lateral organization of these packages define the bed-scale facies associations, assigned to specific depositional environments.

The detailed facies associations analysis showed that the deposits of the Tsotyli Formation in Neapolis-1 are deepwater turbidite facies. More specifically, the marly-mudstone deposits are assigned to inter-lobe facies, while the mudstone-silty facies are distal lobe fringes facies. The sand-dominated facies are mainly lobe or channel facies, while the brecciated interval at the bottom of Tsotyli Formation is

considered to be debritic facies. Although the limestone bedrock is not part of the studied formations, it is considered to be barrier-reef facies.



*Fig.5. Neapolis-1 well synopsis.*



## 5.1 Neapolis-2

### Well synopsis

According to National Hydrocarbon Archive reports (Alexiadis, 1995), Neapolis-2 well was drilled to the eastern flanks of the MHB (**Table 3 and Fig.4**), and penetrated the Tsotyli Formation of Aquitanian-Burdigalian age, and reached the Cretaceous carbonate basement (**Fig.6**).

At this location, the Tsotyli Formation is dominated by alternations of mudstone/marls and argillaceous sandstone, with minor siltstone, breccia and conglomerate deposits. From 0-755m the Tsotyli Formation sediments are grey marls, silty sandstone and sandy conglomerates, while the 755-1030m interval is dominated by marl/mudstone. The Tsotyli Formation interval has two (2) available cores (**See Appendix**). The 1030-1046m interval is the brecciated base of Tsotyli Formation or possibly Pentalofos Formation deposits. The Cretaceous rudist limestone bedrock extends from 1046m to the bottom of the borehole. The bedrock and the transition zone between Tsotyli Formation and bedrock has two (2) available cores, both fully recovered.

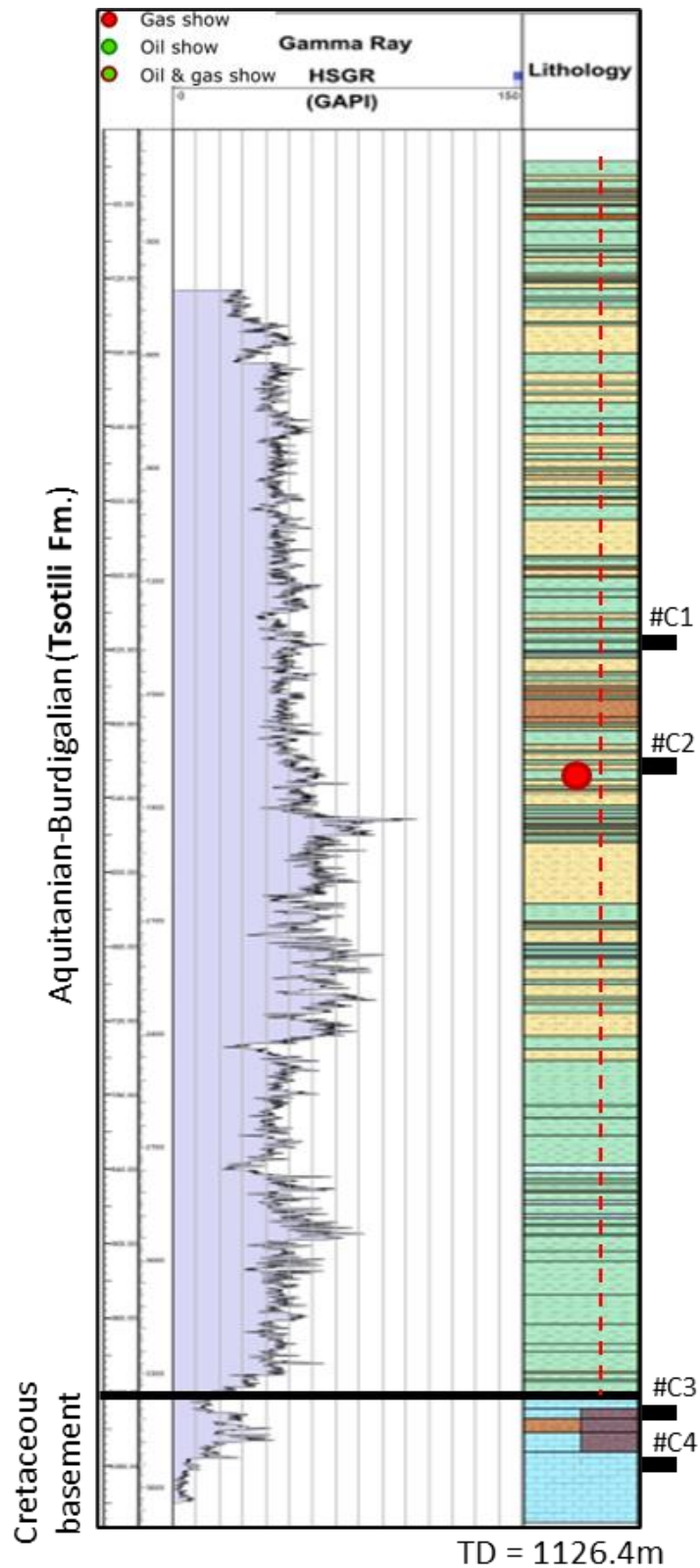
### Facies Associations analysis results

A hierarchical approach to sedimentological description and interpretation has been applied to generate lithotypes through cuttings and core data, which are later grouped to depositional packages with similar characteristics and internal organization. The vertical and lateral organization of these packages define the bed-scale facies associations, assigned to specific depositional environments.

The detailed facies associations analysis showed that Neapolis-2 Tsotyli Fm deposits are deepwater turbidite deposits. More specifically, the marly-mudstone deposits are assigned to inter-lobe facies, while the mudstone-silty facies are distal lobe fringes facies. The sand dominated facies are mainly lobe or channel facies, while the conglomerate facies in Tsotyli Fm interval and the brecciated interval at the bottom of the Formation considered as debritic facies. Although the limestone bedrock is not part of the studied formations, it is considered to be barrier-reef facies.

**Table 3. Neapolis-2 well details**

<b>Basin</b>	Mesohellenic (MHB)
<b>Longitude</b>	21°21'18.71"E
<b>Latitude</b>	40°18'35.78"N
<b>Shows</b>	Gas shows (methane)
<b>Elevation</b>	719.00 m
<b>Operator</b>	IFP
<b>Spud</b>	11.01.1967 - 03.02.1967
<b>Total Depth (TD)</b>	1126.40 m
<b>Available .las files</b>	Gamma Ray (GR), Sonic (DT), Electrical, Spontaneous Potential (SP), Volatile hydrocarbon (S1), (NNTS), Integrated Sonic Transit Time (ITT), Calcimetry
<b>Geochemical information</b>	0-1039m: permanent traces of methane (50-300 ppm)

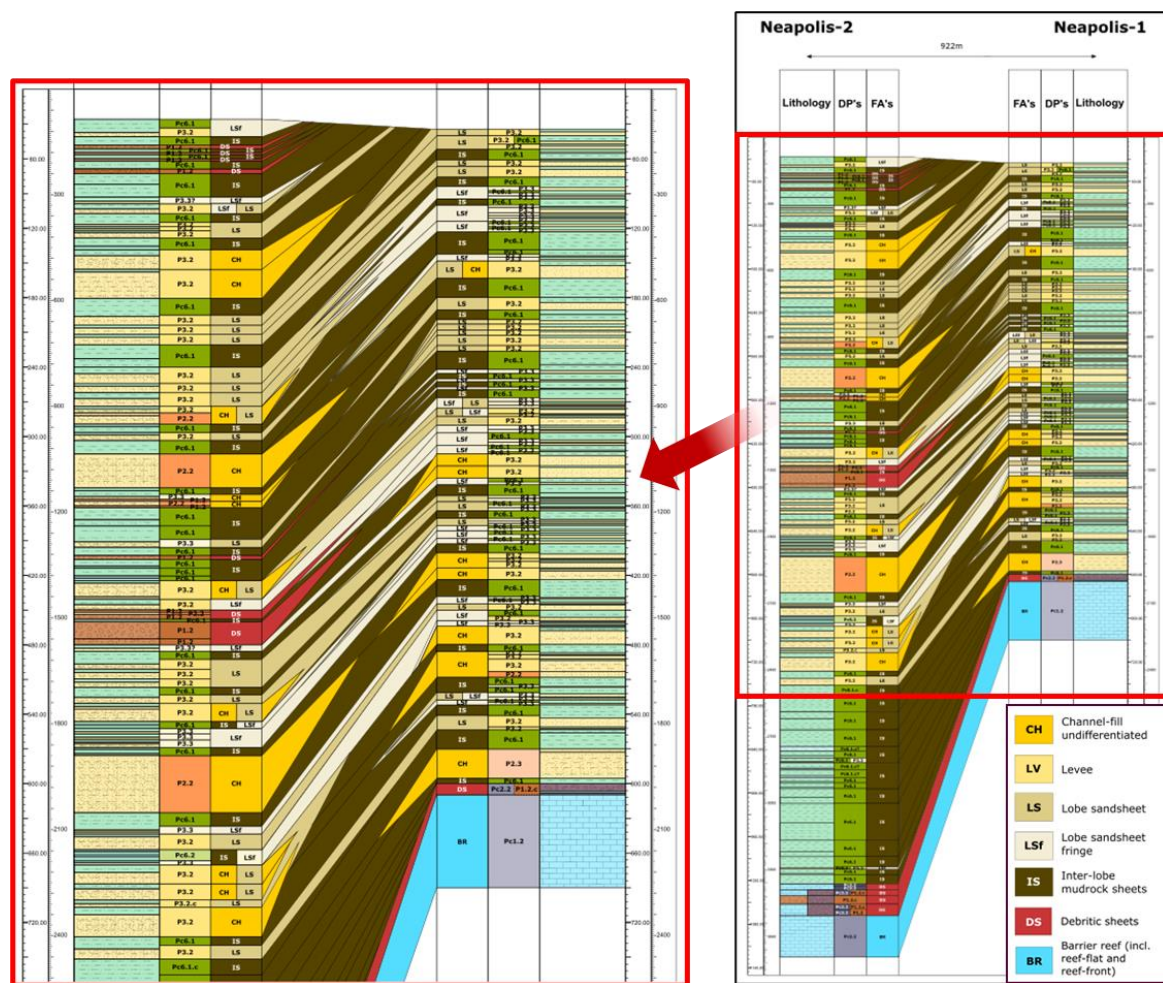


*Fig.6. Neapolis-2 well synopsis.*

### Neapolis-1 and Neapolis-2 wells correlation

The proximity of the two (2) wells (922m), allows an attempt to correlation between the facies associations of Neapolis-1 and Neapolis-2 wells (**Fig.7**).

The dips of the beds suggest a slight displacement of the beds between the two wells, probably due to a normal faulting between the two wells, or due to the dips at the flanks of the MHB. The inter-lobe facies (dark brown on **Fig 7**), which are the dominant ones, are easily traced between the two wells. Thick channel or lobe facies of Neapolis-2 well become thinner in Neapolis-1, thus we see more lobe-fringe facies. Conglomerate debritic sheets of Neapolis-2 are not present in Neapolis-1, probably due to their local nature or the paleogeography (coloured red in Fig. 7). The sand-dominated facies are expected to be lense-shaped, floating among the mudstone dominated inter-lobe facies. Overall, the thick, laterally continuous muddy inter-lobe facies suggest that **Tsotyli Fm could potentially serve as a seal in the MHB.**

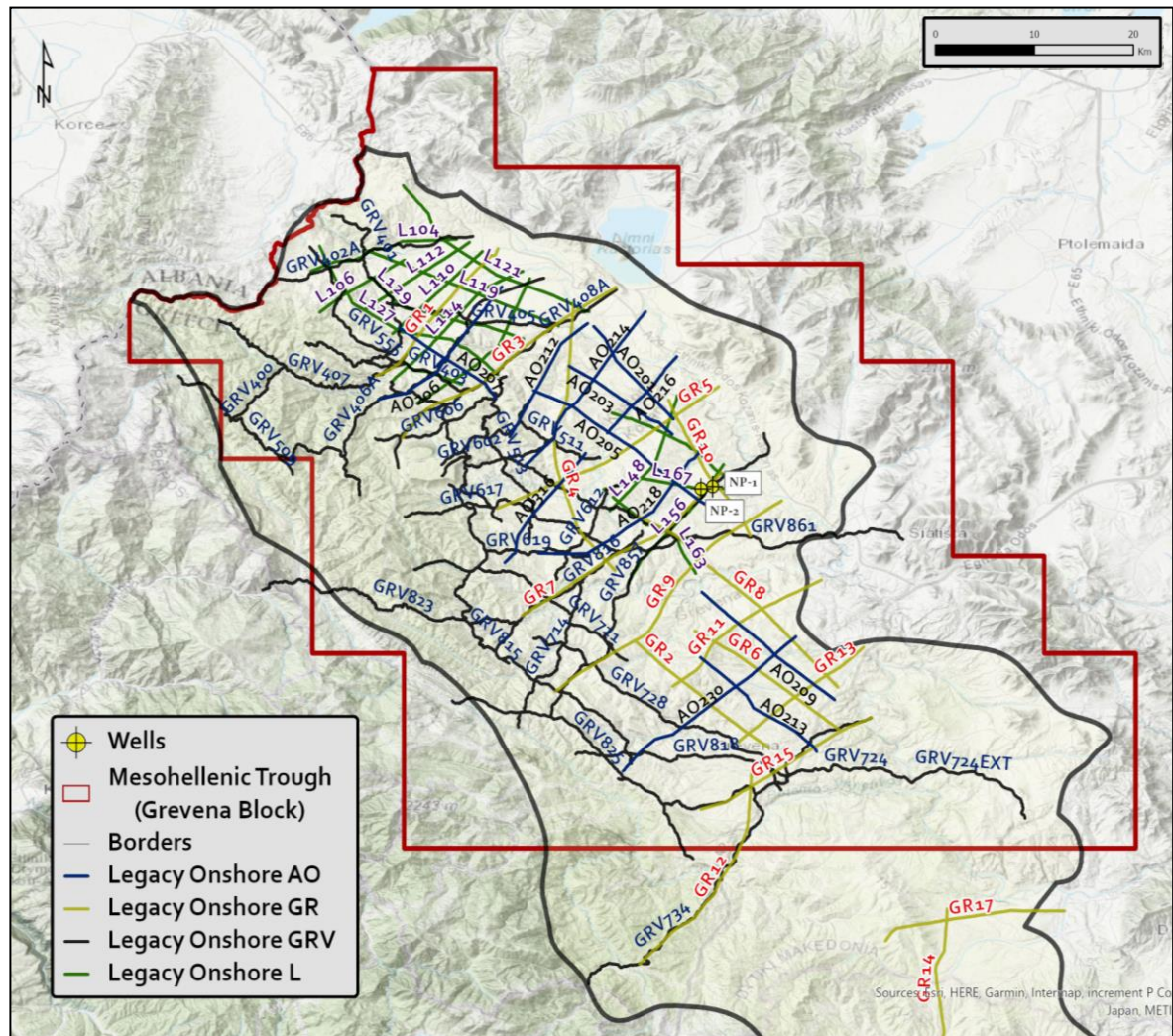


**Fig.7.** Neapolis-1 and Neapolis-2 correlation.

## 6. Legacy Seismic data and interpretation

### 6.1 Geophysical research and available data

Seismic acquisition surveys have been carried out in the area of MHB during the period 1980-1984, 623km of 2D seismic data were acquired with a dynamite source. The seismic campaigns include the GR-lines (1980), the L-lines (1982) and AO-lines (1983) shown in **Figure 8**. During 1991-1994, approximately 662km of 2D seismic data was acquired using a Vibroseis source namely the 'GRV' lines (Figs. 16, 17 and 18).



*Fig.8. Combined legacy seismic campaigns in the area of MHB.*

The available data for this study were from vintage seismic campaigns conducted in the 1990s, which were reprocessed for the PilotSTRATEGY project. HEREMA, in collaboration with the contracted geophysical services provider Geofizyka Toruń (GT), reprocessed the GRV seismic lines acquired during this period (**Fig. 8, 9 and 10**).

The main objective of this re-processing initiative was to improve seismic imaging quality to support structural interpretation and resource assessment. Key goals were:

- Obtaining noise free, high quality 2D seismic data with enhanced signal-to-noise ratio and improved frequency bandwidth,
- Definition of accurate reflector character in terms of vertical and horizontal resolution and continuity,
- Enhancing the overall resolution and continuity of seismic data to properly image the subsurface structures,
- Producing a dataset suitable for detailed structural interpretation and resource assessment.

The dataset for reprocessing consisted of 32 vintage 2D seismic lines, originally acquired between 1991 and 1998 using Vibroseis source technology, covering a total of 662.68 km. The reprocessing effort was completed within six months and employed state-of-the-art seismic processing techniques to generate a high-quality pre-stack time-migrated (PSTM) broadband dataset.

The processing up to pre-stack time migration was executed using the SeisSpace software of Halliburton-Landmark, GLI Hampson-Russell, SUMMIG and VELANAL software of Techco Geophysical Services Ltd., along with Geofizyka Toruń's proprietary tools and procedures. These processes were carried out in accordance with high international standards and the best geophysical processing practices. Advanced algorithms were employed to significantly enhance the signal-to-noise ratio, reduce noise, and improve reflector continuity, as evident in the improved seismic sections (see **Figs. 11, 12 and 13**).

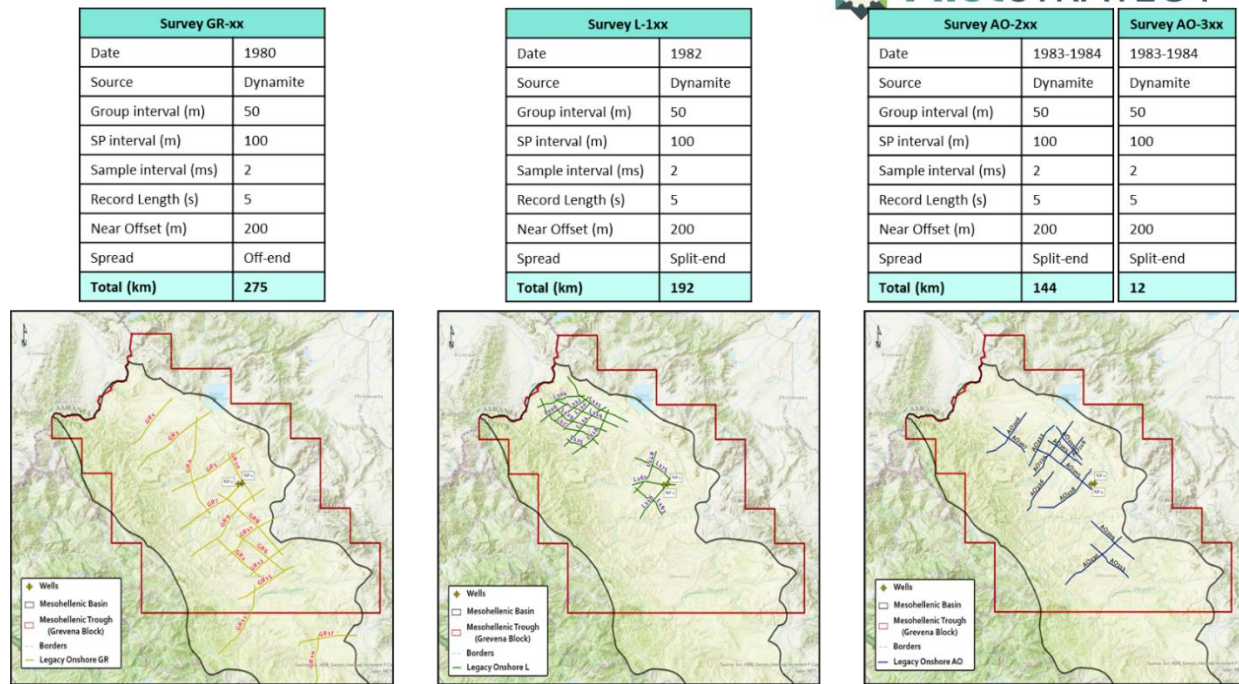


Fig.9. Legacy seismic survey campaigns with a dynamite source, in the area of MHB and their shooting parameters.

Survey GRV-4xx		Survey GRV-5xx	Survey GRV-6xx	Survey GRV-7xx	Survey GRV-8xx
Date	1991-1994	1991-1994	1991-1994	1991-1994	1991-1994
Source	Vibroseis	Vibroseis	Vibroseis	Vibroseis	Vibroseis
Group interval (m)	40	40	40	40	40
SP interval (m)	40	40	40	40	40
Sample interval (ms)	4	4	4	4	4
Record Length (s)	5	5	5	5	5
Near Offset (m)	180	180	180	180	180
Spread	Symmetrical	Symmetrical	Symmetrical	Symmetrical	Symmetrical
<b>Total (km)</b>	<b>131</b>	<b>96.44</b>	<b>79.12</b>	<b>147.84</b>	<b>208.28</b>

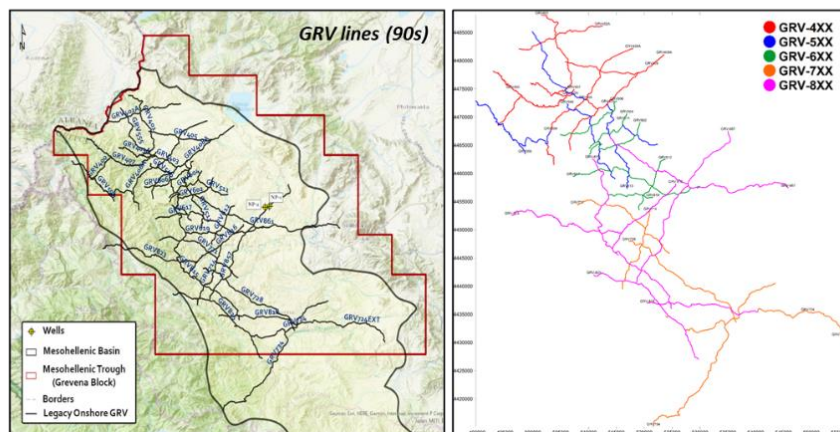
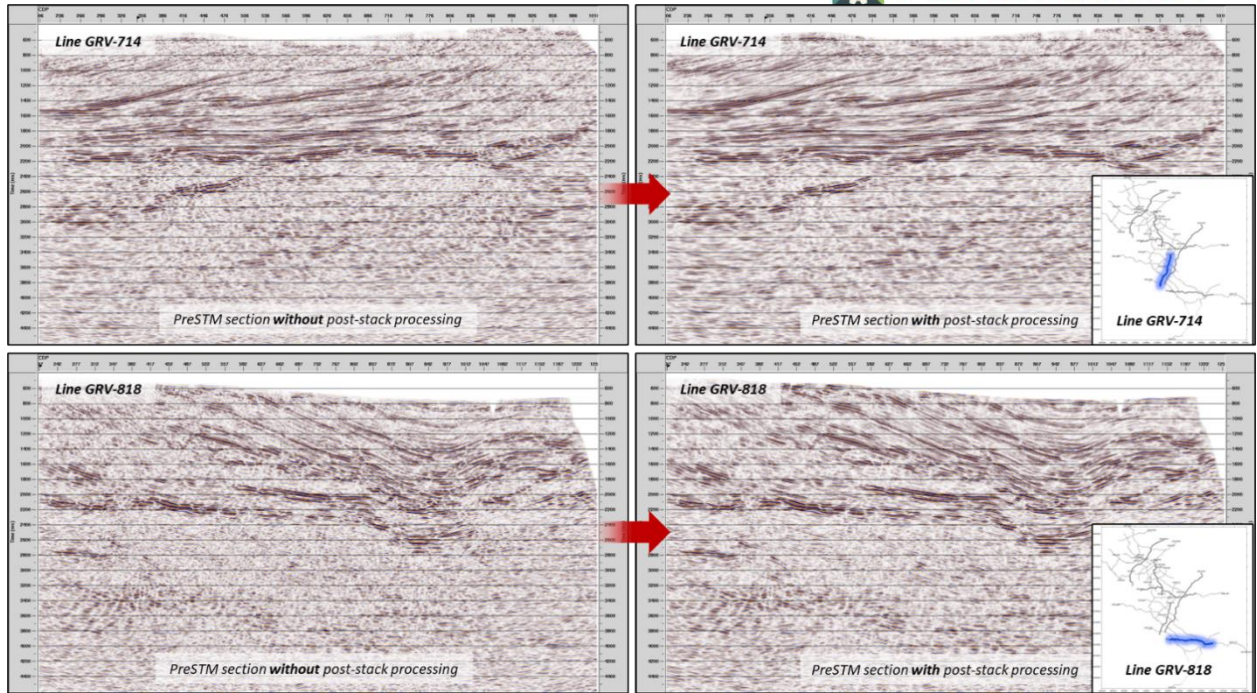
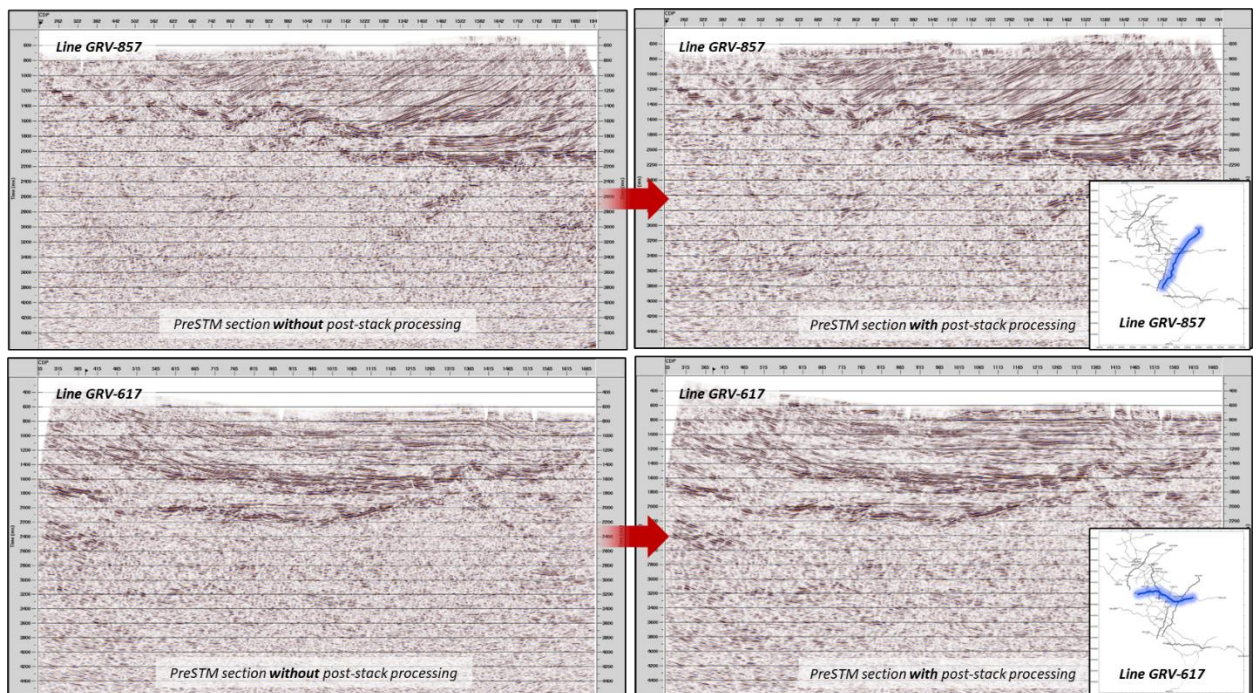


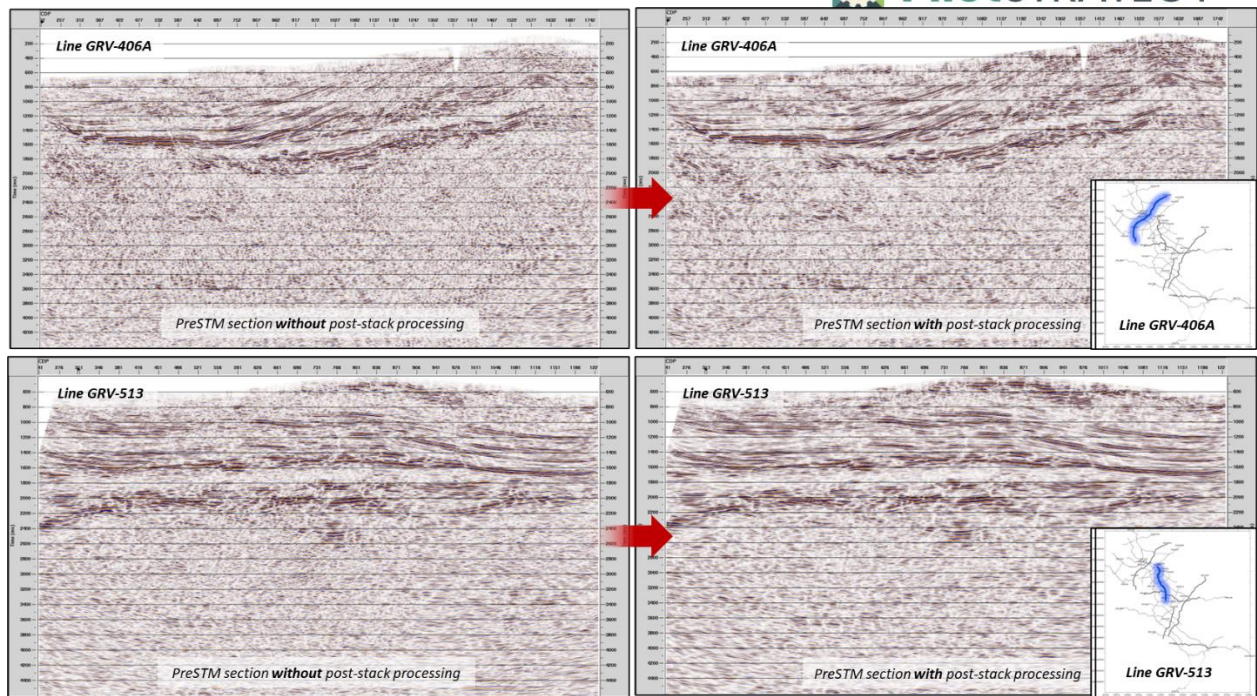
Fig.10. Legacy seismic survey campaigns using a Vibroseis source, in the area of MHB and their shooting parameters.



**Fig.11.** Examples of PreSTM section before and after post-stack processing. Presented sections are generated with dynamic amplitude scaling (AGC).



**Fig.12.** Examples of PreSTM section before and after post-stack processing. Presented sections are generated with dynamic amplitude scaling (AGC).



**Fig.13.** Examples of PreSTM section before and after post-stack processing. Presented sections are generated with dynamic amplitude scaling (AGC).

## 6.2 Interpreted horizons

The following horizons were interpreted.

- **Ground surface (H1):** The ground surface corresponds to the first strong reflector. However, as we are dealing with land data, there is a lack of continuity in acoustic impedance contrast across the basin, and even in some cases, there are data gaps that are more prominent at the surface due to gaps in the placement of sources and/or receivers. These variations are commonly attributed due to the complex hilly terrain and the weathered rock/sediment layers close to the surface. To address these variations, static corrections have been applied.
- **Top Pliocene-Pleistocene (H2):** Represents the upper boundary of Pliocene-Pleistocene sediments, predominantly observed in the northern and northwestern parts of the MHB, where it is commonly exposed at the surface.
- **Top Ondria Formation (H3):** Marks the upper boundary of the Ondria Fm, which is mainly observed locally in areas of the northern part of MHB, often exposed at the surface.
- **Top Tsotyli Formation (H4):** Represents the upper boundary of the Tsotyli Fm, which is mainly present in the northern part of MHB, often exposed at the surface.
- **Top Pentalofos Formation (H5):** Represents a regionally continuous horizon corresponding to the upper boundary of the Pentalophos Fm. The formation is well exposed across the MHB, thus we are confident that the horizon is representing the top of Pentalofos formation
- **Top Eptachori Formation (H6):** Represents the uppermost layer of the Eptachori Fm and is

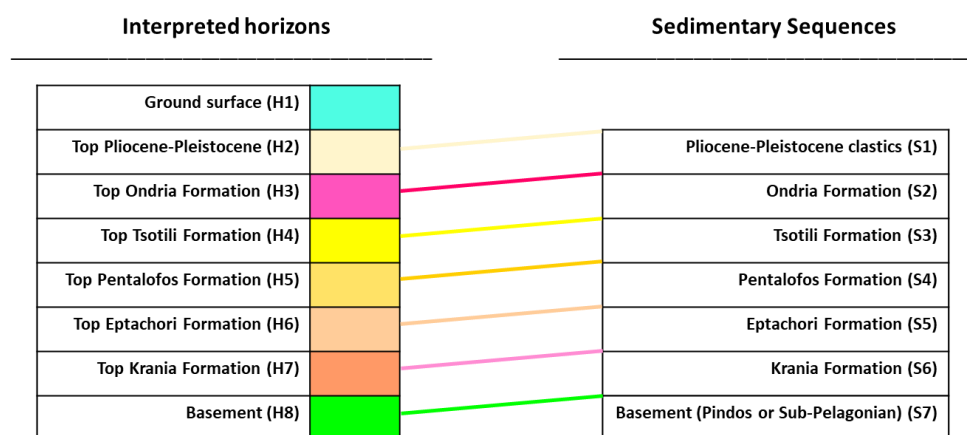


regionally continuous.

- The formation is exposed at the surface of the MHB; thus, we are confident that the horizon is representing the top of Eptachori formation.
- **Top Krania Formation (H7):** A regionally observed horizon, possibly associated with the top of Eocene and the upper boundary of the Krania Fm. It is mainly observed in the eastern parts of the MHB, where it onlaps the next identified horizon-H8, corresponding to the basement.
- **Basement (H8):** Represents the base of the Eocene clastic sediments, which often rests unconformably on the underlying Alpine basement. It is a regional marker and can be traced across the entire MHB.

The main formations identified in the study area are H4-H8, which have been regionally mapped and presented further in Chapters 6.4 and 6.5. Horizons H2 and H3 have not been mapped, due to their limited presence within the seismic data. Horizon H4, corresponding to the Tsotyli Fm), is mainly observed in the northern part of the seismic dataset, thus the mapping effort has been focused in this area (**Fig.22**).

For the regional seismic interpretation, it was important to identify the key reflectors and delineate the principal sequences (**Fig.14**):



*Fig.14. Interpreted Horizons (left panel) and sequences (right panel) indicated with colours.*

### 6.3 Seismic sequence and facies

The sequences (**Fig.15**) described below are based on the seismic character of each sedimentological domain within the study area. The siliciclastic domain consists of six (6) distinct facies (S1-S6, **Fig. 15**), while the carbonate domain of the basement is represented by facies (S7, **Fig.15**).

S1: Pliocene-Pleistocene clastics, mostly sandy conglomerate, with lense shaped clay beds and lignite beds. These deposits are present mainly to the eastern parts of the MHB basin, in Grevena area. Younger sediments, including alluvial fan deposits, are assigned to S1 sequence. Thickness: 200-300m.

S2: Ondria Formation; consists of early to mid-Miocene sandstones and marls with interbedded fossiliferous limestone layers. Thickness: >350m.

S3: Tsotyli Formation; characterised by early mid-Miocene marls interbedded with sandstones in the northern parts of the MHB, and gneissic pebbles rich conglomeratic beds in the southern areas. Thickness: approx. 600m.

S4: Pentalofos Formation; Late Oligocene and early Miocene sandstone beds coarsening upwards into conglomeratic beds; mainly conglomeratic beds in the southern parts of the MHB. Thickness: up to 2,500m.




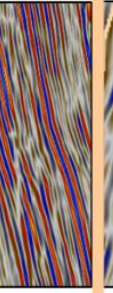
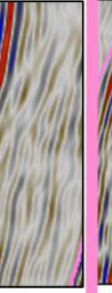
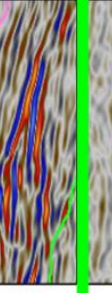
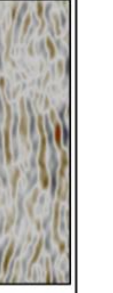
S5: Eptachori Formation; Oligocene deposits dominated by silty marls in the upper part of the formation with decimetric thick very fine sandstone beds often overlying on thick conglomerates in the lower part. Thickness: up to 1,000m.

S6: Krania Formation; Eocene deposits dominated by shales with massive sandstone interbeds, locally overlying conglomerates and limestones. The latter host a benthic macrofossil fauna. Thickness up to 1,500m.

S7: The Basement exhibits distinct lithological variations across the study area:

To the East: The Triassic to Middle Jurassic crystalline limestones, locally overlain by Upper Jurassic Ophiolites of the Sub-Pelagonian.

To the West: the Pindos Middle to Upper Cretaceous rudist and marly brecciated limestones. Upper Jurassic Ophiolites are also locally present.

Sequence	Reflection Configuration	Amplitude	Frequency	Continuity	Interpretation	Example
S1	Parallel continuous to semi-continuous	High	High/Moderate	High	Pliocene-pleistocene clastics	
S2	Parallel continuous	High	Moderate	High	Ondria Fm. Turbidites	
S3	Parallel semi-continuous with transparent reflections	Moderate	High/Moderate	Moderate	Tsotili Fm. Turbidites	
S4	Parallel continuous	High	Low	High	Pentalofos Fm. Turbidites	
S5	Parallel semi-continuous with transparent reflections	Low	Low	Moderate	Eptachori Fm. Turbidites	
S6	Parallel continuous to semi-continuous. Locally	High	Low	High	Krania Fm. Turbidites	
S7	Contorted to chaotic with transparent reflections	Low	Low	Low/Moderate	Carbonate basement	

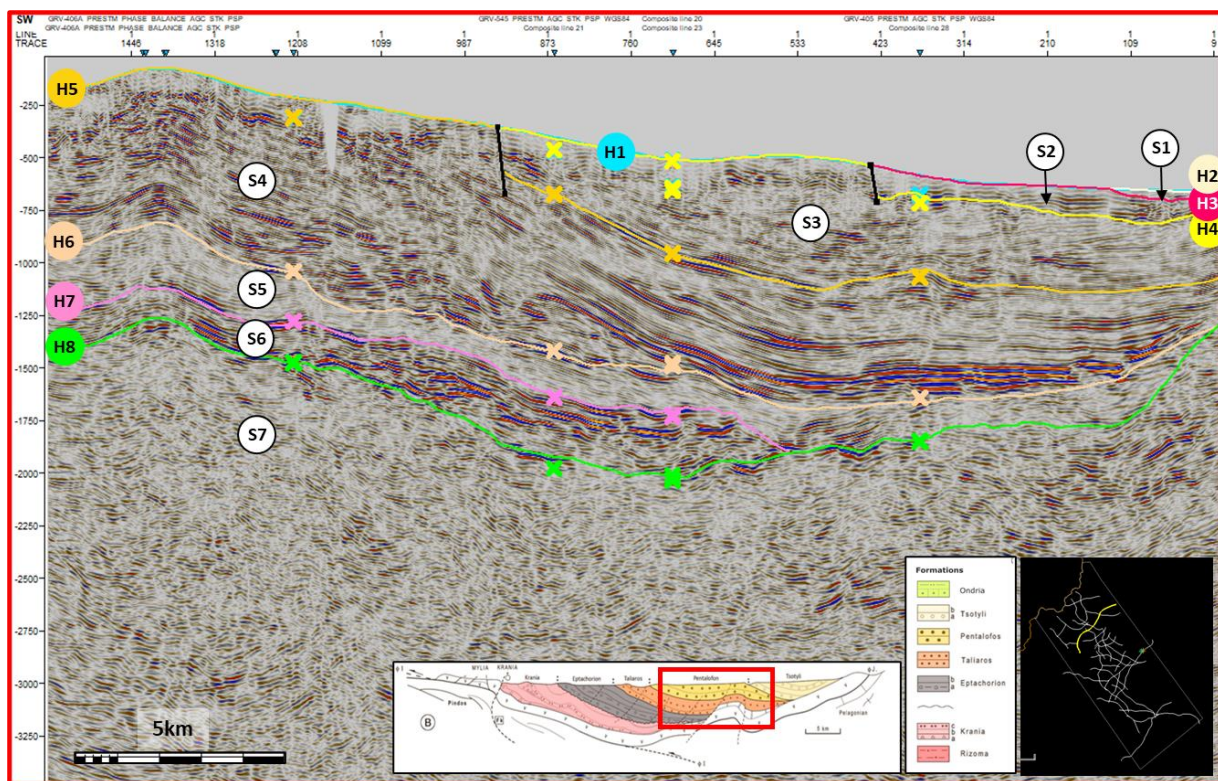
*Fig.15. Seismic facies overview of the MHB.*

## 6.4 Regional seismic interpretation

### Seismic line GRV-406A

**Figure 16** illustrates a NE-SW (left to right) section across the MHB. It is easy to distinguish the “U” shape of the basin floor (H8 horizon-Basement) in the SW-NE orientation. This section depicts all identified horizons (H1-H8) and sequences (S1-S7).

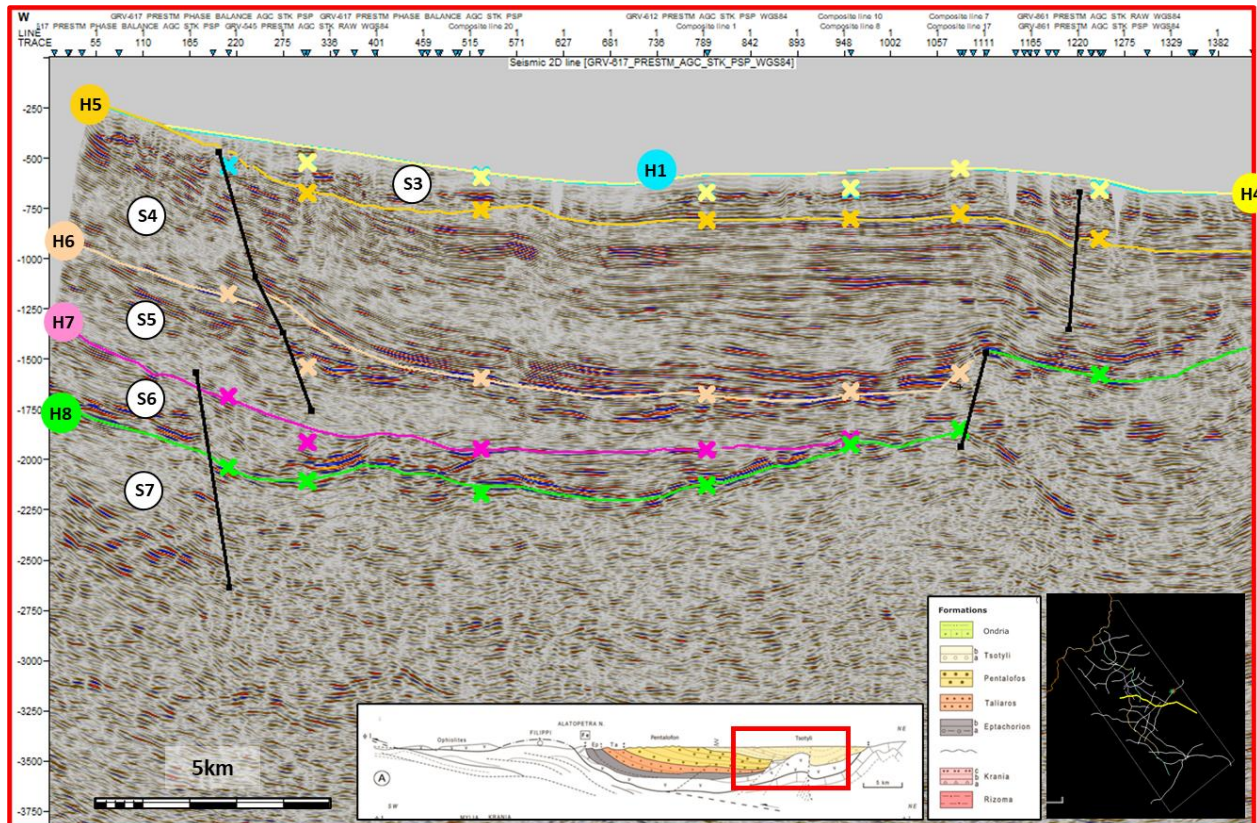
The Krania Fm deposits (S6) pinch-out against the basement towards the SW. Overlying these deposits, the Eptachori Formation (S5) extends towards the SW but similarly pinches out against the basement in the NE direction. Above S5, the Pentalofos Formation (S4) shows significant localized thickening in the SW, where it is exposed at the surface. Further, the overlying Tsotyli Fm (S3), Ondria Fm (S2) and Pliocene-Pleistocene deposits are exposed at the surface in the NE areas. S3 is significantly thicker compared to S2 and S1 in this line. Normal faults are evident throughout the seismic sections and across the basin, locally offsetting the stratified beds and disrupting the continuity of the sequences.



**Fig.16.** Regional interpreted seismic profile running from SW-NE. The profile’s location is shown on the inset map, alongside the previously published geological model by Ferrière et al. (2013), Zeliidis et al. (2002) and Kontopoulos et al. (1999).

### Seismic line GRV-617

**Figure 17** illustrates a W-E oriented seismic section, depicting the pinch-out sequences S6, S5 and S4 onto the basement, as the section progresses towards the eastern margin of the MHB. This seismic profile highlights all identified horizons (H4-H8) and sequences (S3-S7). The S6-S3 sequences form a wedge-shape sedimentary package, tilting westward due to the geometry and tectonic setting of basement and the westward sediment source. Normal faults traversing the basin locally, creating discontinuities within the sedimentary layers.

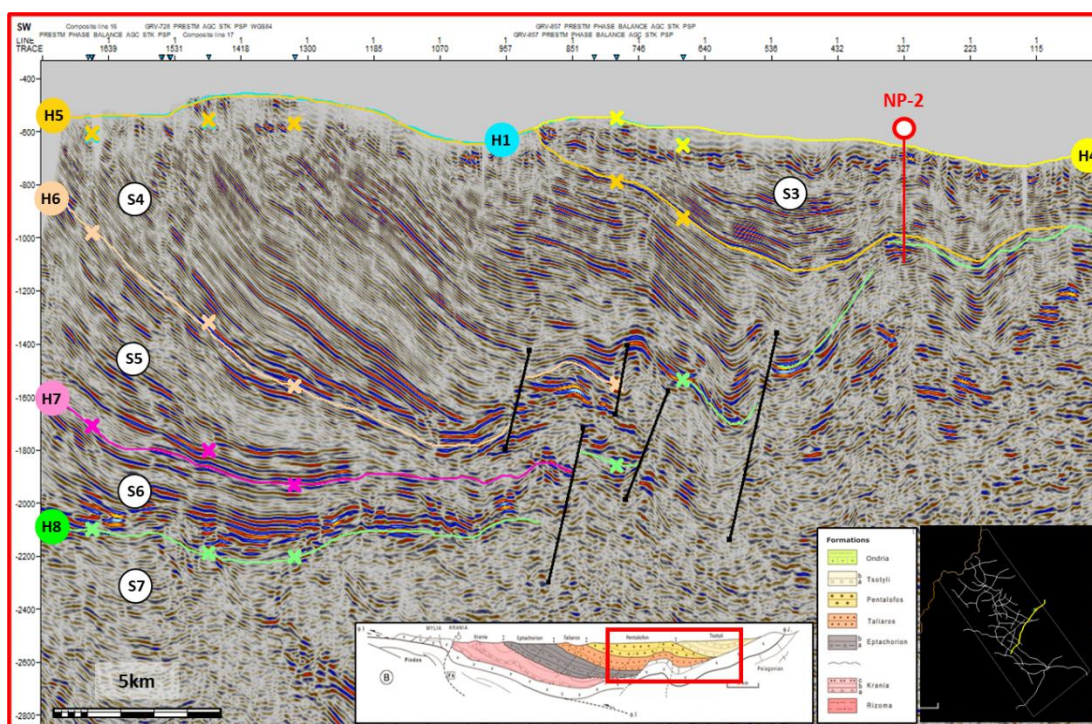


**Fig. 17:** Regional interpreted seismic profile running from W-E. The profile's location is shown on the inset map, alongside the previously published geological model by Ferrière et al. (2013), Zelilidis et al. (2002) and Kontopoulos et al. (1999).

### Seismic line GRV-857

**Figure 18** illustrates a SW-NE seismic section, highlighting the pinch-out of the S6, S5 and S4 sequences onto the basement, as the profile progress toward the eastern margin of the MHB. All identified horizons (H4-H8) and sequences (S3-S7) are clearly presented along this line. The sequences S6-S3 form a wedge-shape package of sediments, tilting due to the underlying basement geometry and the westward source of sedimentation.

The NP-2 well is projected onto the line and its interpretation (see Chapter 3.1), indicates that the well penetrates the S3 sequence, reaching the basement at a depth of 1126.4m. Within the 1030-1046m interval of the NP-2, the deposits are identified as the brecciated base of the Tsotyli Fm or potentially deposits of the Pentalofos Formation. The presence of Pentalofos Formation deposits in this section remains uncertain; however, the interpretation depicts the H5 horizon pinching out on the H8 horizon.

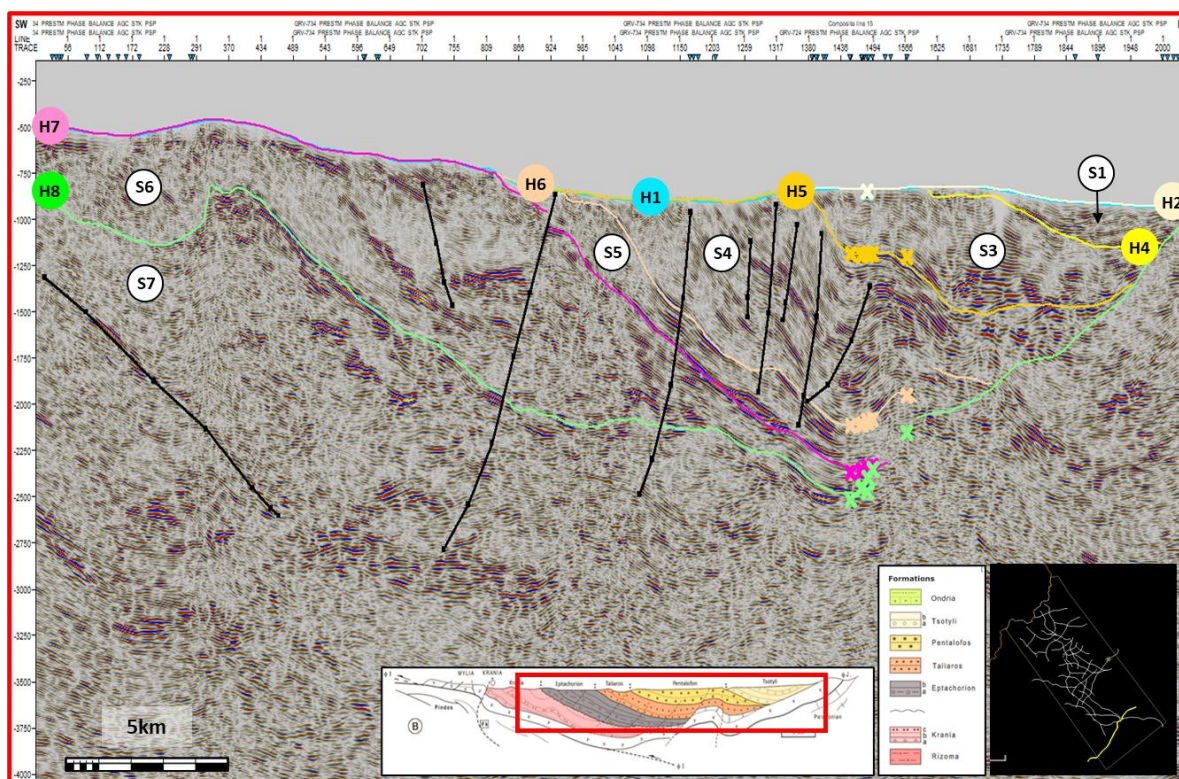


**Fig. 18:** Regional interpreted seismic profile running from SW-NE. Projected NP-2 well to the NE part of the seismic profile, penetrated Tsotyli Formation, possibly Pentalofos Formation and reached the Pelagonian limestone basement. The profile's location is shown on the inset map, alongside the previously published geological model by Ferrière et al. (2013), Zelilidis et al. (2002) and Kontopoulos et al. (1999).

## Seismic Line GRV-734

Seismic line GRV-734 (**Fig.19**) has a SW-NE orientation and was selected to illustrate the geometry of the formations towards the depocenter and southern part of the MHB. Similar to 617 and 857 seismic lines, this line depicts the pinch-out of the S6-S1 sequences against the basement, as we approach the NE margin of the MHB. This line clearly depicts all the identified horizons (H1-H8) and sequences (S1-S7).

The S6-S1 sequences form a wedge-shape package of sediments that tilts to the west, influenced by the underlying basement geometry, and the source of sedimentation to the west. Notably, at this location, the MHB is approximately 35 km wide, providing an opportunity to observe the entire basin from SW to NE. Normal faults within the basin create favorable conditions for structural traps, particularly in the internal regions of the basin.

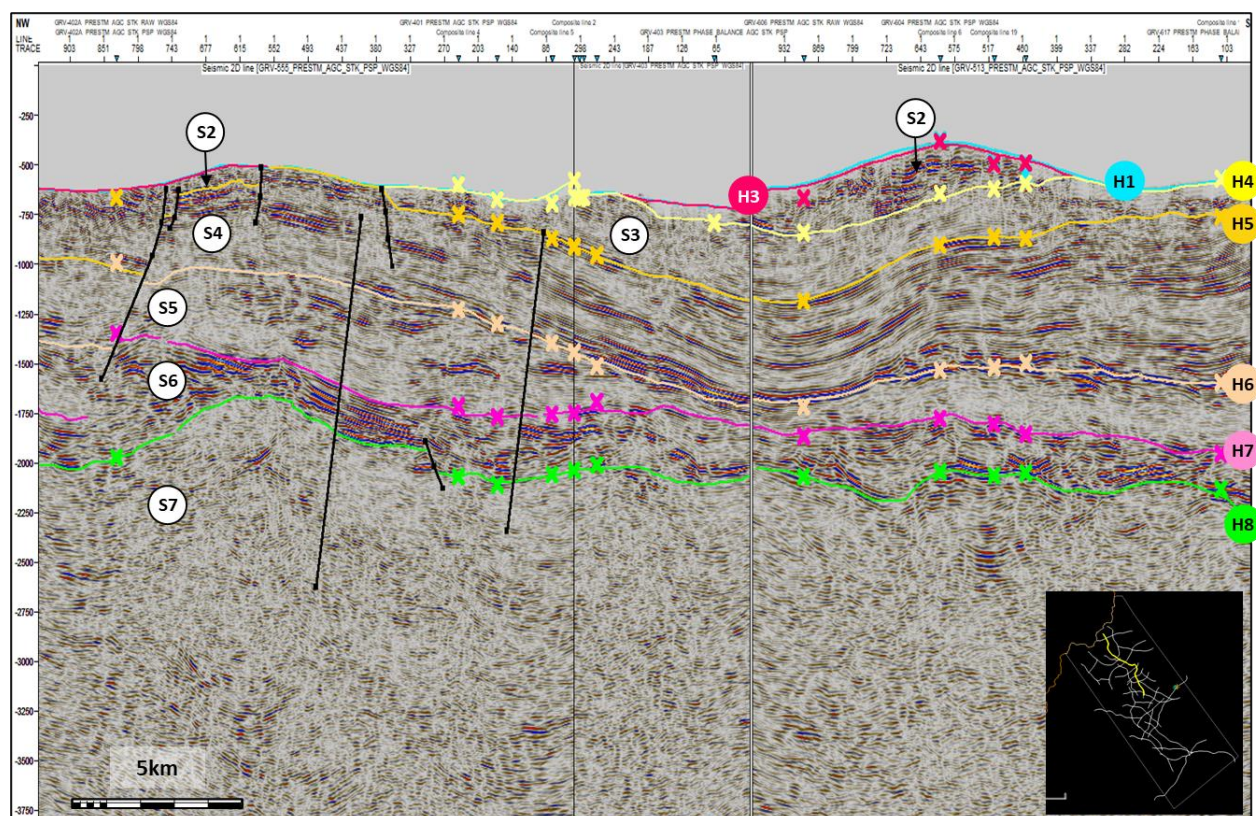


**Fig. 19:** Regional interpreted seismic profile running from SW-NE. The profile's location is shown on the inset map, alongside the previously published geological model by Ferrière et al. (2013), Zeliidis et al. (2002) and Kontopoulos et al. (1999)

## Composite Seismic Lines GRV-555 & 403 & 513

**Figure 20** shows a NW-SE oriented composite line, illustrating the vertical geometry of the stratigraphic formations across the central part of MHB. This profile illustrates all identified horizons, except H2. As anticipated, the S6-S2 sequences are showing a stacking pattern, while S1 is absent from this line but it is observed further to the east. The wavy geometry of these sequences suggests the potential for structural-anticline traps, while the faults may give rise to structural-fault traps. Anticlinal folding creates possible structural-anticline traps, while the faulting observed in this section is indicative of potential fault-controlled traps.

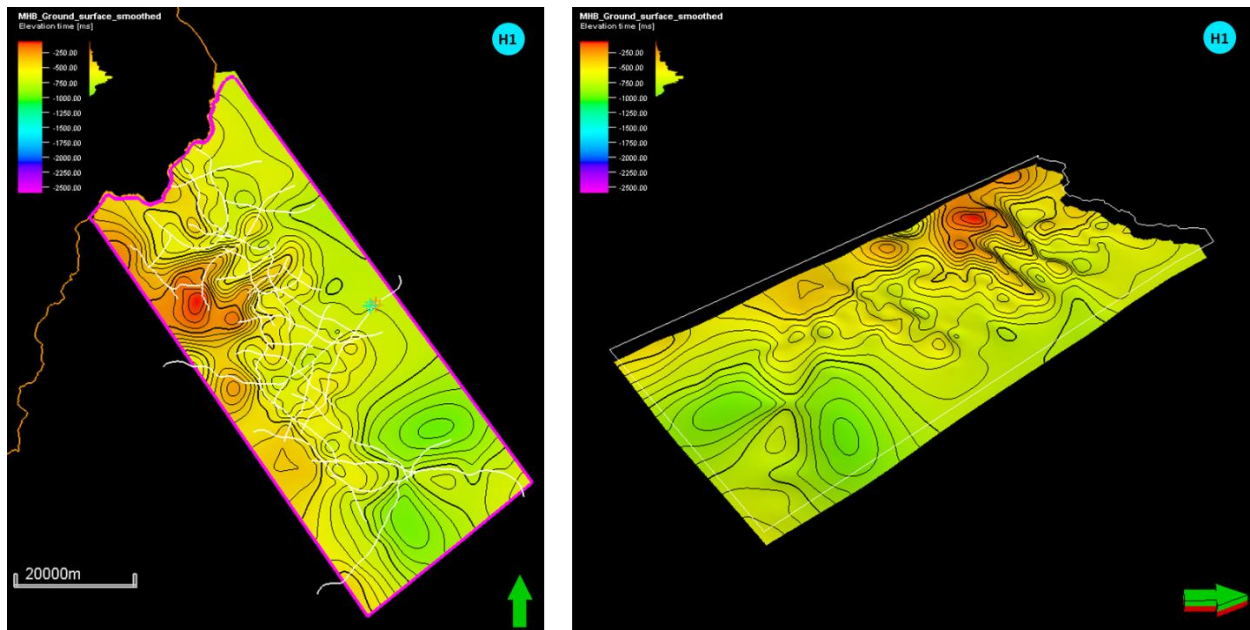
A notable feature is the wedge-shaped geometry formed by the sequences S6 to S1, which dip westward due to the underlying basement's tilting geometry and sediment supply predominantly originating from the west. This tilting is consistent with basin subsidence patterns and sedimentary filling mechanisms. A notable feature is the wedge-shaped geometry formed by the sequences S6 to S1, which dip westward due to the underlying basement's tilting geometry and sedimentary filling mechanisms. In this segment, the basin spans approximately 35 km in width, allowing a comprehensive view of the formations continuity from SW to NE. Normal faults, clearly observed cutting through the sequence boundaries, act as both structural traps and (perhaps) as pathways for potential fluid migration within the basin.



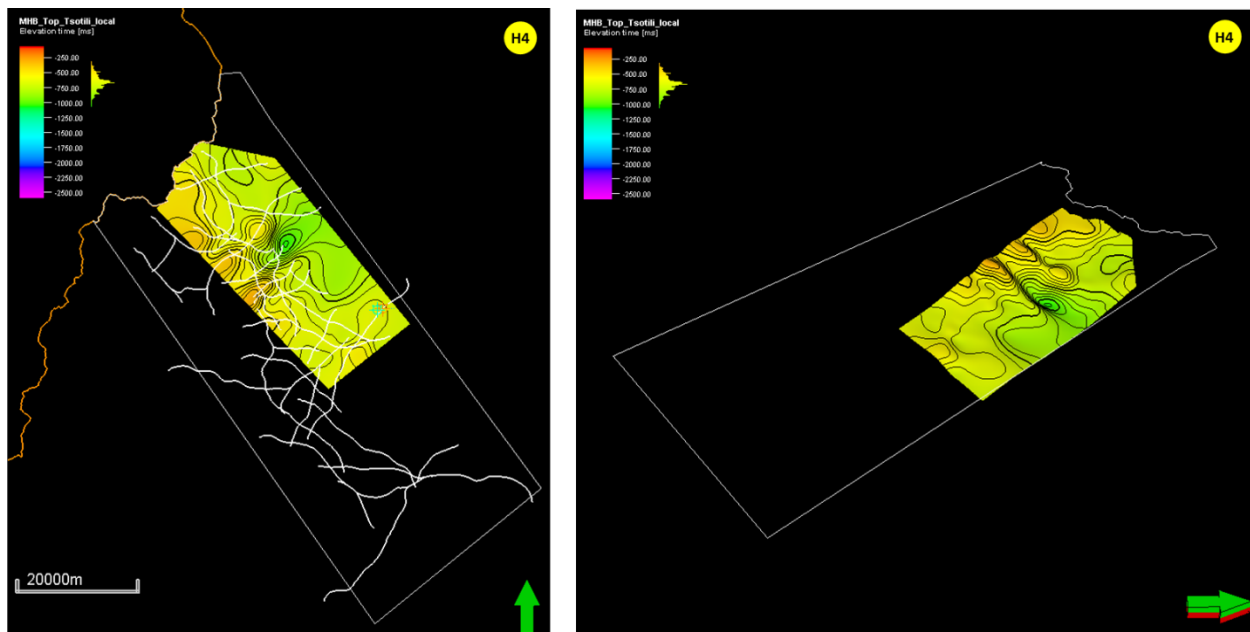
*Fig. 20: Regional interpreted seismic profile running from NW-SE.*



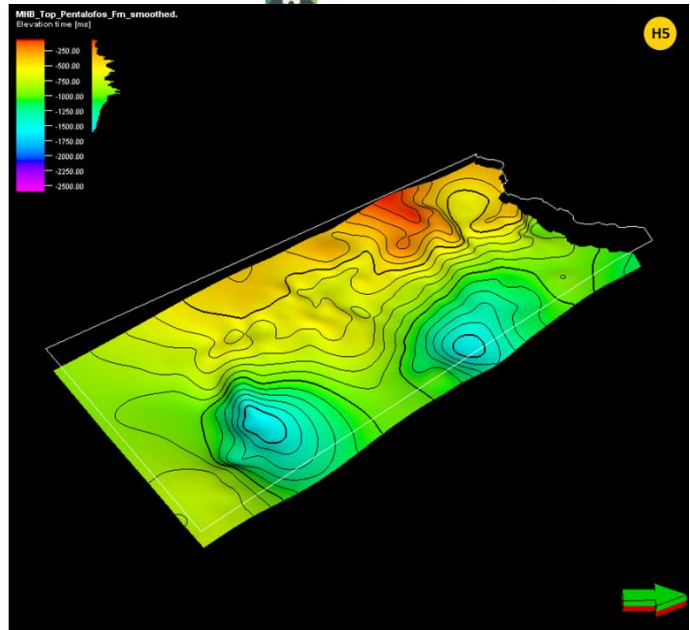
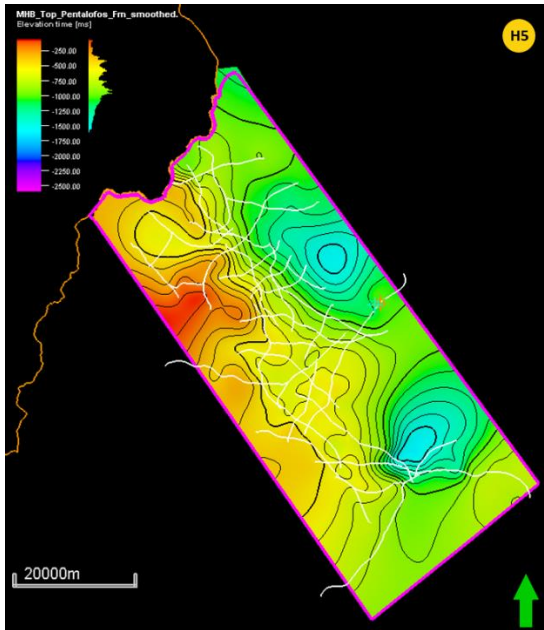
## 6.5 Regional Mapping & traps



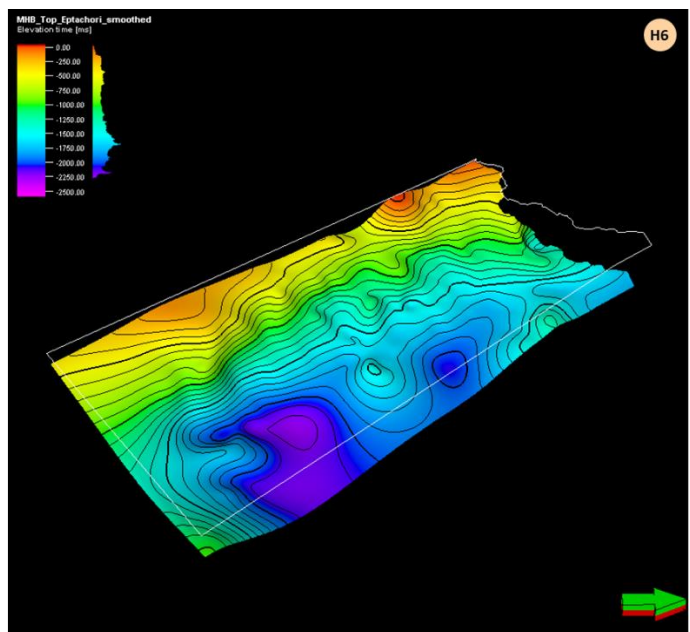
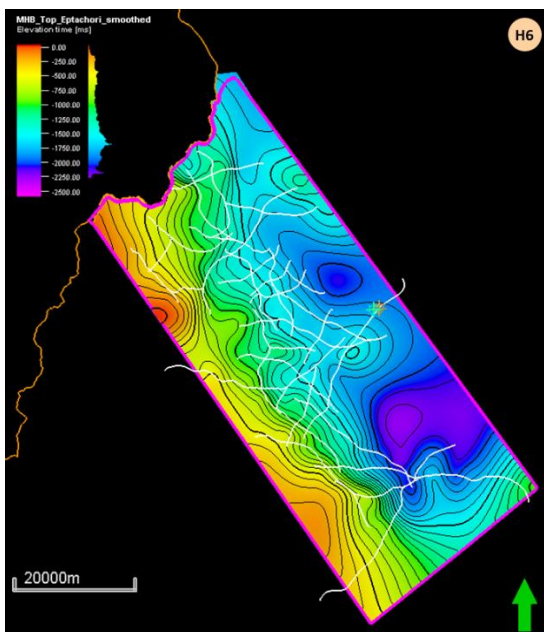
**Fig.21.** H1-Ground surface map based on 2D regional interpreted seismic lines, in MHB (left: 2D view, right: 3D view).



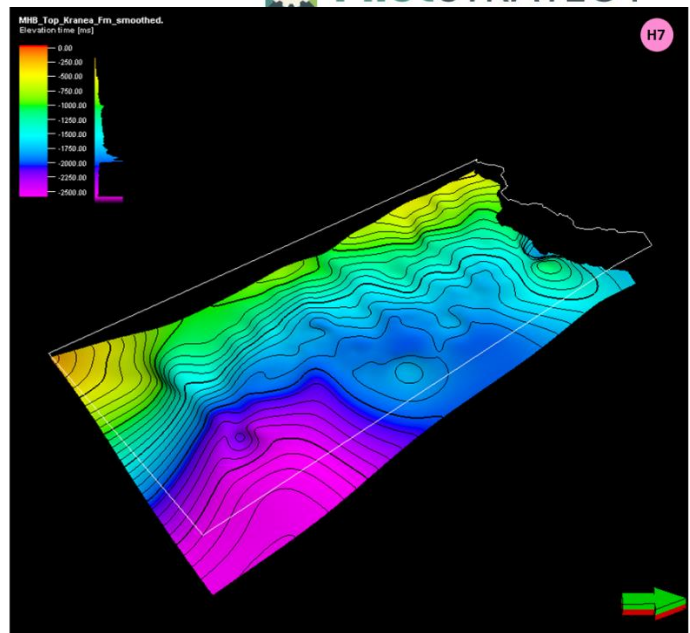
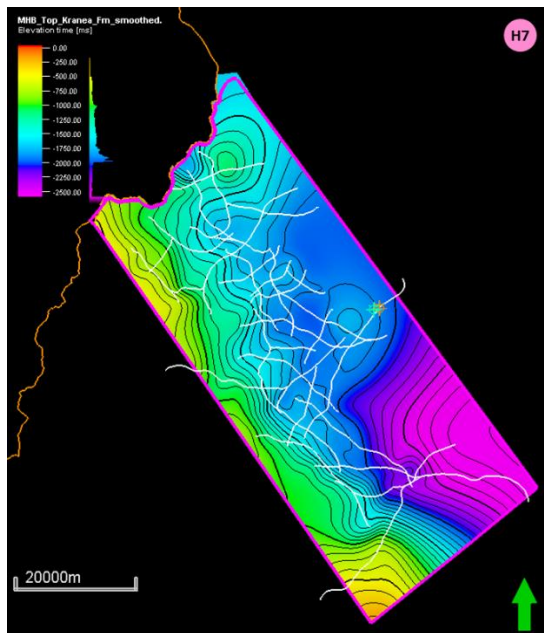
**Fig.22.** H4-Top Tsotyli Formation map based on 2D regional interpreted seismic lines, in MHB (left: 2D view, right: 3D view).



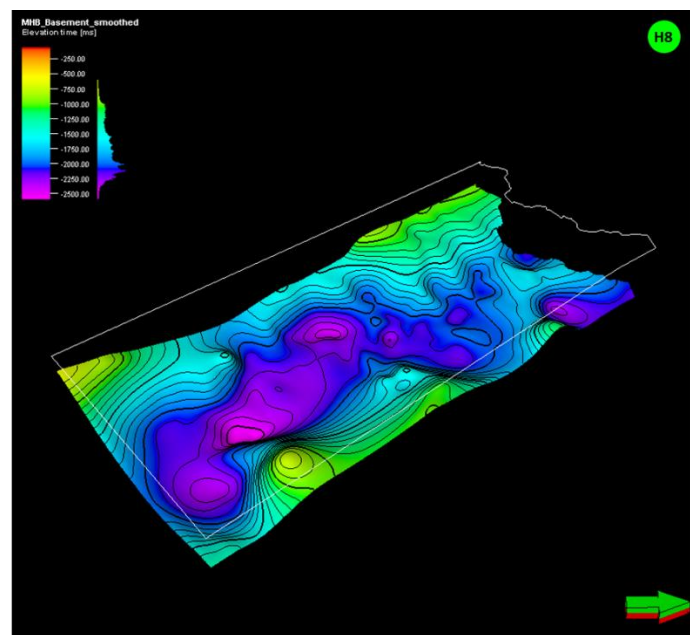
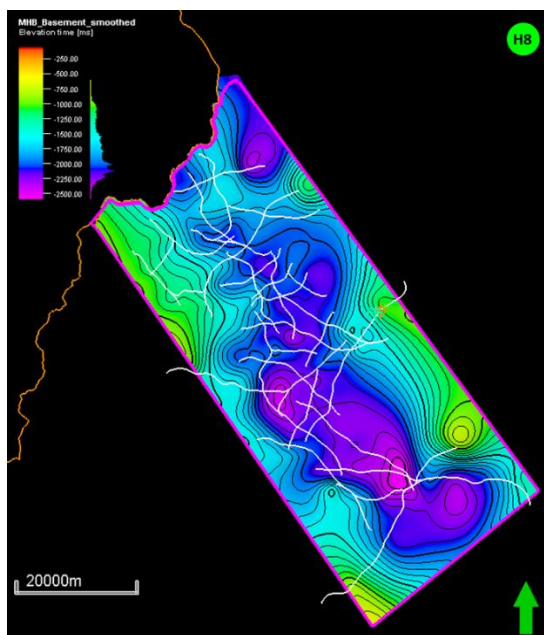
**Fig.23.** H5-Top Pentalofos Formation map based on 2D regional interpreted seismic lines, in MHB (left: 2D view, right: 3D view).



**Fig.24.** H6-Top Eptachori Formation map based on 2D regional interpreted seismic lines, in MHB (left: 2D view, right: 3D view).



**Fig.25.** H7-Top Kranea Formation map based on 2D regional interpreted seismic lines, in MHB (left: 2D view, right: 3D view).



**Fig.26.** H8-Basement map based on 2D regional interpreted seismic lines, in MHB (left: 2D view, right: 3D view).

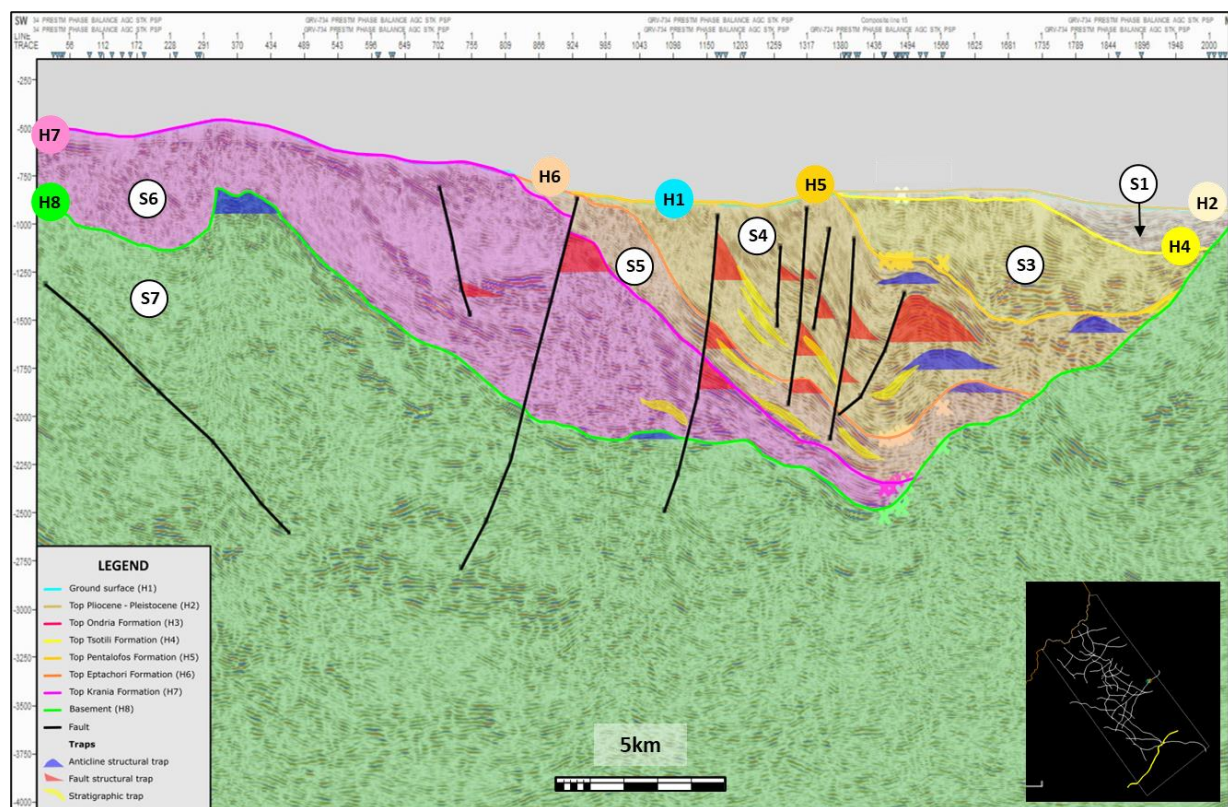
## Traps

Based on the seismic interpretation and regional mapping conducted, several areas of interest for potential traps have been identified. **Figure 27** provides an overview of representative structural and stratigraphic traps derived from the interpretation of the re-processed seismic data.

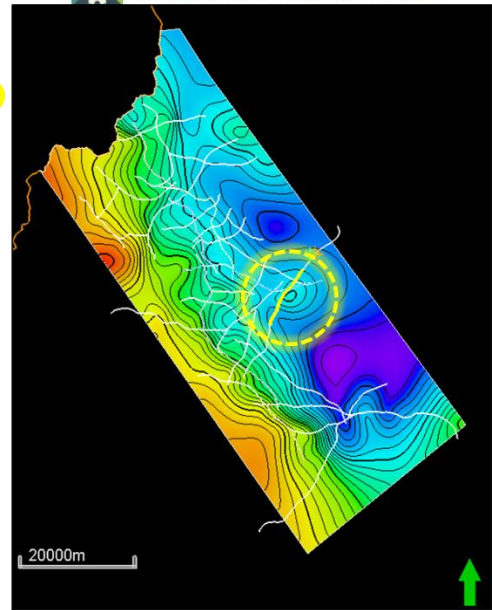
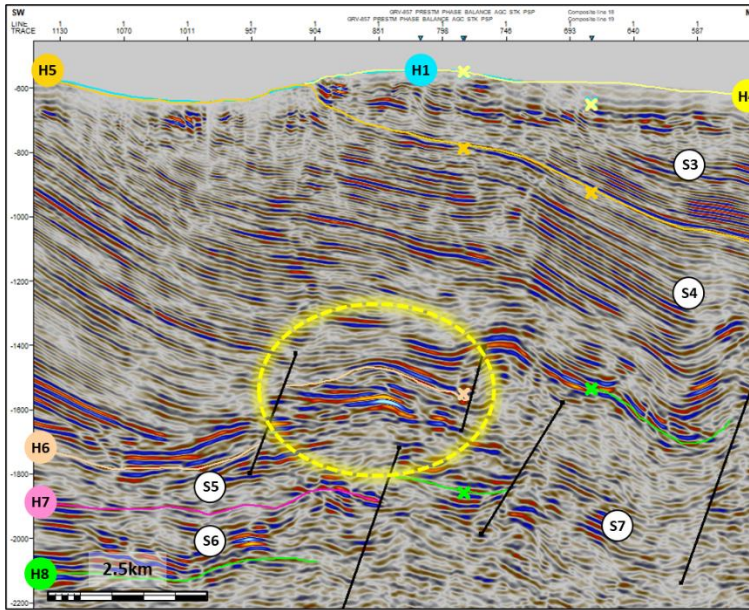
Anticlinal structural traps (Figures 27 and 28) are typically 1–2.5 km in width, with relatively low relief (<500 m). These features are predominantly observed within the S7–S4 sequences and, in some cases, occur in association with stratigraphic traps, either stacked or in direct contact.

Fault-related structural traps are particularly prevalent within the MHB, especially in the S6–S4 sequences, due to the abundance of buried normal faults (**Figures 28, 29, and 30**). These traps are generally small in scale but frequently appear stacked across multiple seismic profiles (Figure 36).

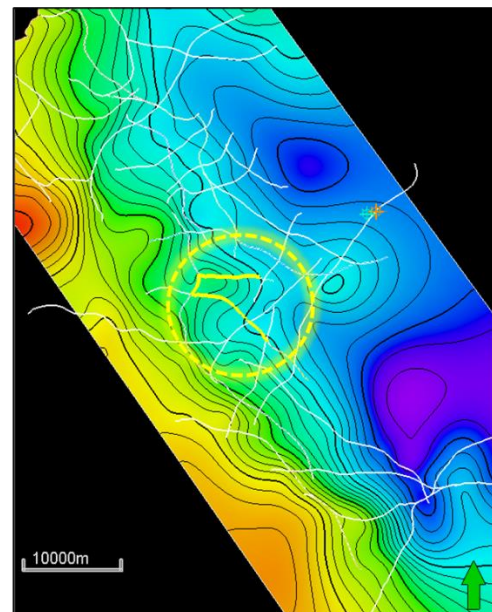
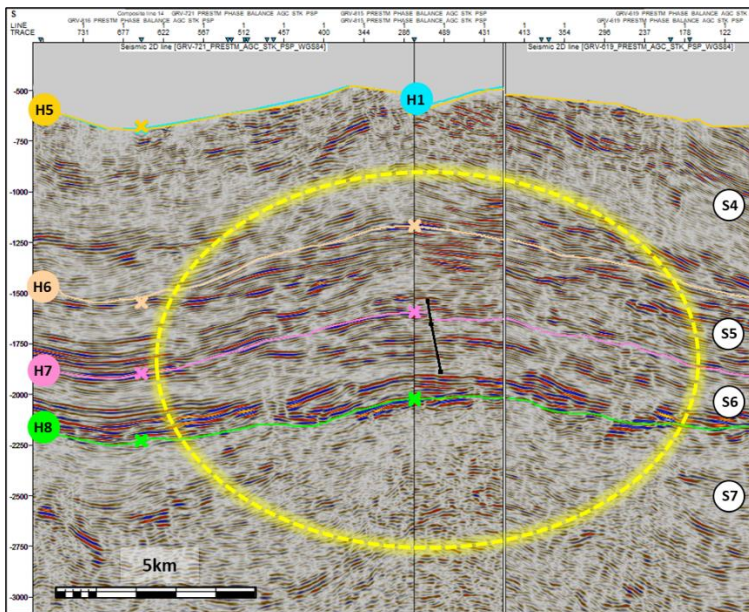
Stratigraphic traps, including submarine-fan traps and pinch-out traps (**Figure 27**), exhibit significant lateral extent and are often stacked. However, these traps are characterized by relatively small thicknesses.



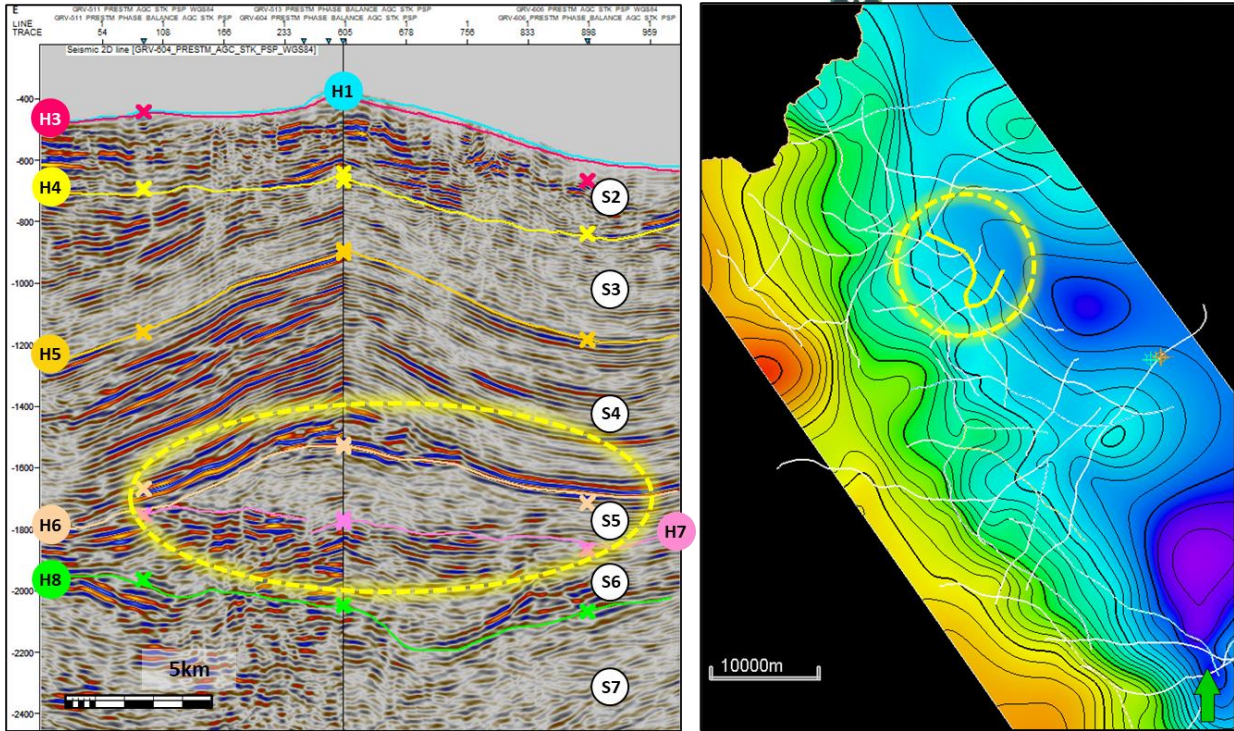
**Fig.27.** Regional interpreted seismic profile running from SW-NE, with possible structural (blue and red colours) and stratigraphic (yellow colour) traps.



**Fig.28.** Possible anticline trap, on the interpreted seismic profile (left) and the Top Eptachori Formation map (right) based on 2D regional interpreted seismic lines, in MHB.



**Fig.29.** Possible local structural trap, on the interpreted seismic profile (left) and the Top Eptachori Formation map (right) based on 2D regional interpreted seismic lines, in MHB



**Fig.30.** Possible local structural trap identified on the interpreted seismic profile (left) and the Top Eptachori Fm map (right), based on 2D regional seismic interpretation within the MHB.

## 7. Conclusions

This study presents a detailed seismic interpretation of the Mesohellenic Basin (MHB) offering new insights into the basin's stratigraphy, structural framework, and sedimentological evolution. Key findings include the identification and mapping of significant horizons and sequences, as well as the characterisation of potential structural and stratigraphic traps that enhance our understanding of the region's geological history and resource potential.

The comprehensive reprocessing of seismic data using advanced techniques has significantly improved the resolution and continuity of subsurface imaging, allowing for the delineation of eight key horizons and associated sedimentary sequences. These results have not only reinforced existing geological models but have also clarified the relationship between tectonic activity, sedimentation and basin evolution. Notably, the analysis highlights the interplay between the eastern and western sediment sources, as well as the tectonically driven variations in deposition patterns across the basin.

This study has also underscored the presence of promising structural traps, including anticline and fault-related traps, particularly within the Krania, Eptachori, and Pentalofos formations. These features, along with stratigraphic traps such as pinch-outs and submarine fans, present opportunities for further exploration and assessment of the basin's CO<sub>2</sub> storage potential. The identification of thick, laterally extensive seal units within the Tsotyli Fm further supports the suitability of the MHB for subsurface resource storage.

Despite these advancements, the study also reveals areas where additional data acquisition and analysis are needed to resolve uncertainties. For instance, the chronostratigraphy of certain formations, as well as the lateral continuity of key reflectors, remains a challenge due to lack of well data information and the inherent complexity of the basin. Future efforts should focus on integrating additional geophysical and geological data, including integration of vintage 1980s seismic data, to refine the structural and stratigraphic framework.

## 8. References

- Alexiadis, Ch. (1995). Preliminary petroleum geology report of the Mesohellenic Trough. PPC (DEP-EKY) unpublished report.
- Brunn, J. H. (1956). Contribution a l'etude geologique du Pinde Septentrional et d'une partie de la Macedoine occidentale. Laboratoire de geologie de l'Universite.
- Brunn, J. H. (1960). Geological Map of Greece, Pentalophos Sheet, scale 1: 50 000. IGEY, Athens.
- Decourt, J., Aubouin, J., & Savoyat, E. (1977). Le sillon mesohellenique et la zone pelagonienne. Bull. Soc. Geol. Fr, 1, 32-70.
- Desprairies, A. (1979). Etude sédimentologique de formations à caractère flysch et molasse, Macédoine, Epire (Grèce). Mem. Soc. Géol. France, 136, 1-80.
- Doutsos, T., Pe-Piper, G., Boronkay, K. T., & Koukouvelas, I. (1993). Kinematics of the central Hellenides. Tectonics, 12(4), 936-953.
- Doutsos, T., Koukouvelas, I., Zelilidas, A., & Kontopoulos, N. (1994). Intracontinental wedging and post-orogenic collapse in the Mesohellenic Trough. Active Continental Margins—Present and Past, 257-275.
- Ferrière, J., Reynaud, J. Y., Pavlopoulos, A., Bonneau, M., Migiros, G., Chanier, F., Proust, J-N., & Gardin, S. (2004). Geologic evolution and geodynamic controls of the Tertiary intramontane piggyback Meso-Hellenic basin, Greece. Bulletin de la Société géologique de France, 175(4), 361-381.
- Ferrière, J., Chanier, F., Reynaud, J., Pavlopoulos, A., Ditbanjong, P., & Coutand, I. (2013). Evolution of the Mesohellenic Basin (Greece): a synthesis. Ed.) Emmanuel Skourtsos, The Geology of Greece. Part II, Journal of the Virtual Explorer, Electronic Edition. ISSN, 1441-8142.
- Kontopoulos, N., Fokianou, T., Zelilidis, A., Alexiadis, C., & Rigakis, N. (1999). Hydrocarbon potential of the middle Eocene-middle Miocene Mesohellenic piggy-back basin (central Greece): A case study. Marine and Petroleum Geology, 16(8), 811-824.
- Koukouzas, N., Krassakis, P., Koutsovitis, P., & Karkalis, C. (2019). An integrated approach to the coal deposits in the Mesohellenic Trough, Greece. Bulletin of the Geological Society of Greece, 54(1), 34-59.
- Koumantákīs, I., & Matarangas D. (1980). Geological map of Greece: Panayia sheet. Institute of Geology and Mineral Exploration.
- Ori, G. G., & Roveri, M. (1987). Geometries of Gilbert-type deltas and large channels in the Meteora Conglomerate, Meso-Hellenic basin (Oligo-Miocene), central Greece. Sedimentology, 34(5), 845-859.
- Robertson, A. H. F., Dixon, J. E., Brown, S., Collins, A., Morris, A., Pickett, E., Sharp, I., & Ustaömer, T. (1996). Alternative tectonic models for the Late Palaeozoic-Early Tertiary development of Tethys in the Eastern Mediterranean region. Geological Society, London, Special Publications, 105(1), 239-263.
- Savoyat E., Lalechos N., Philippakis N. & Bizon G. (1972a). – Geological map Kalambaka Sheet, 1:50,000. – IGME, Athens.



Savoyat E., Monopolis D. & Bizon G. (1971a). – Geological map Nestorion Sheet, 1:50,000. – IGME, Athens.

Savoyat E., Monopolis D. & Bizon G. (1972b). – Geological map Grevena Sheet, 1:50,000. – IGME, Athens.

Savoyat E., Verdier A., Monopolis D. & Bizon G. (1971b). – Geological map Argos Orestikon Sheet, 1:50,000. – IGME, Athens.

Savoyat, E., & Lalechos, N. (1969). Geological Map of Greece, scale 1: 50 000, Trikala Sheet.

Vamvaka, A., Kiliyas, A., Mountrakis, D., & Papaoikonomou, J. (2006). Geometry and structural evolution of the Mesohellenic Trough (Greece): a new approach. Geological Society, London, Special Publications, 260(1), 521-538.

Wilson, J. W. (1993). Origin and tectono-stratigraphic evolution of the Meso-Hellenic Trough, Northern Greece and Albania. KB thesis scanning project 2015.

Wilson, J. (1993). The anatomy of the Krania basin, north-west Greece. Δελτίον της Ελληνικής Γεωλογικής Εταιρίας, 28(1), 361-368.

Zelilidis, A., & Kontopoulos, N. (1997). Depositional environments of the Pentalophos formation in the Mesohellenic basin: Application to the concept of the hydrocarbon habitat. MINERAL WEALTH-ATHENS-, 45-52.

Zelilidis, A., Kontopoulos, N., Avramidis, P., & Bouzos, D. (1997). Late Eocene to early Miocene depositional environments of the Mesohellenic basin, North-Central Greece: implications for hydrocarbon potential. Geologica Balcanica, 27, 45-56.

Zelilidis, A., Piper, D. J. W., & Kontopoulos, N. (2002). Sedimentation and basin evolution of the Oligocene-Miocene Mesohellenic basin, Greece. Aapg Bulletin, 86(1), 161-182.

Zygojiannis, N., & Müller, C. (1982). Nannoplankton-Biostratigraphie der tertiären Mesohellenischen Molasse (Nordwest-Griechenland). Zeitschrift der Deutschen Geologischen Gesellschaft, 133(3), 445-455



## APPENDIX

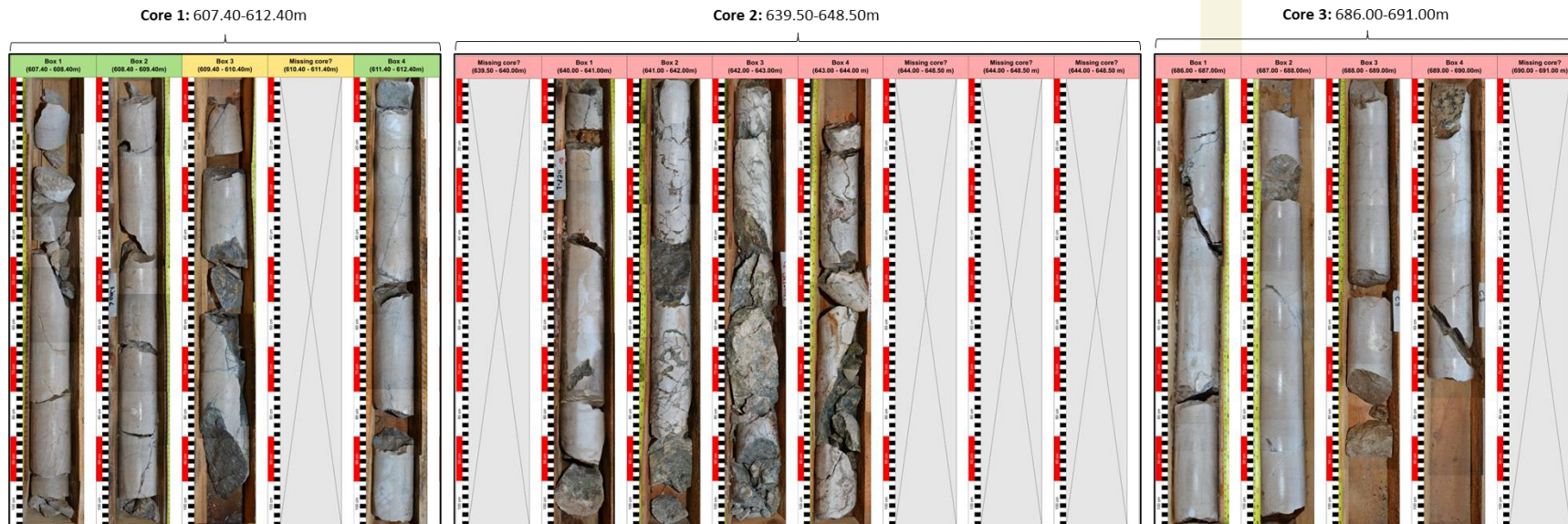


**Core data**

Core #1: 607.00-612.00m, recovered 5.00m (100%)  
 Core #2: 639.00-648.50m, recovered 9.50m (100%)  
 Core #3: 686.00-691.00m, recovered 5.00m (100%)

**Confidence about the core position/order**

- High
- Medium
  - no labels but signs of matching with vintage data
  - contradicts vintage data and other boxes
- Low
  - no labels
  - severe reposition of core in box
  - Complete mismatch with vintage data
  - Missing core/box issues



Core photos from Neapolis-1 well in MHB. Notice that all cores have been taken from the basement section. Box colours assigned depending on the confidence of core position and order; green for high, yellow for medium and red for low confidence.

The PilotSTRATEGY project has received funding from the European Union’s Horizon 2020 research and innovation programme under grant agreement No. 101022664



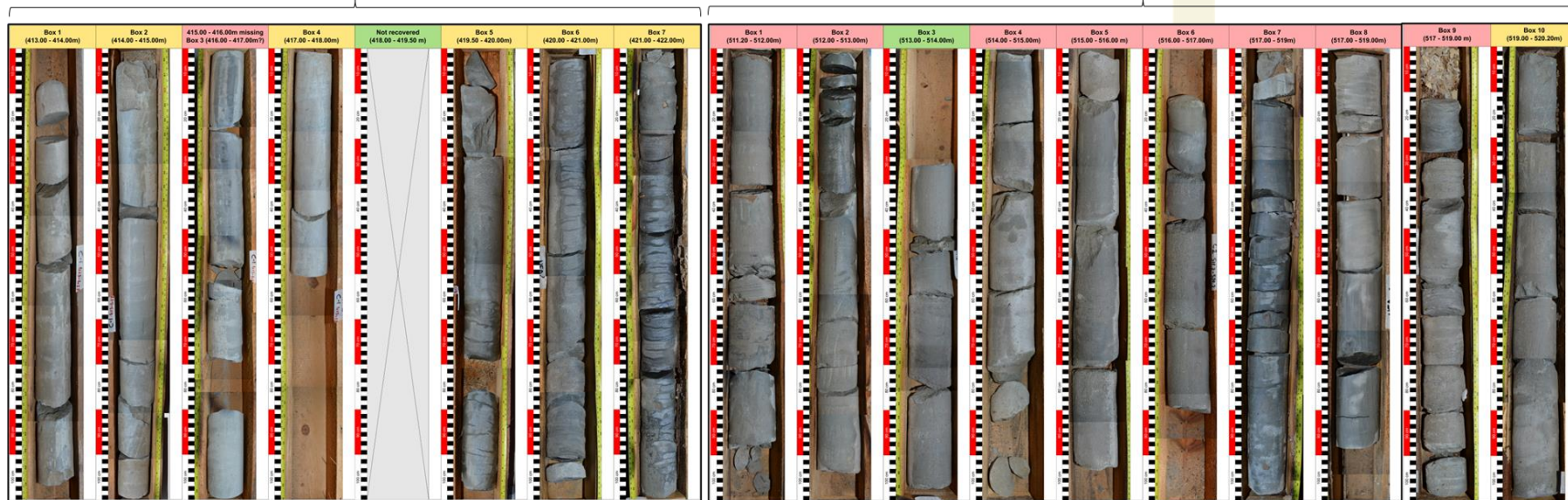
### Core data

Core #1: 413.00-422.00m, recovered 7.70m (86%)  
 Core #2: 511.20-520.20m, recovered 9.00m (100%)  
 Core #3: 1036.00-1040.00m, recovered 5.00m (100%)  
 Core #4: 1075.30-1080.30m, recovered 5.00m (100%)

Confidence about the core position/order	
■	High
■	Medium
<ul style="list-style-type: none"> <li>• no labels but signs of matching with vintage data</li> <li>• contradicts vintage data and other boxes</li> </ul>	
■	Low
<ul style="list-style-type: none"> <li>• no labels</li> <li>• severe reposition of core in box</li> <li>• Complete mismatch with vintage data</li> <li>• Missing core/box issues</li> </ul>	

Core 1: 413.00-422.00m (Tsotili Fm. inter-lobe facies)

Core 2: 511.20-520.20m (Tsotili Fm. lobe facies)



Core photos from Neapolis-2 well in MHB. Cores #1 and #2 have been taken from Tsotyli Formation interval. Core #1 marly deposits with thin sandstone laminations assigned as inter-lobe facies, while core #2 sand dominated facies belong to a turbidite lobe system. Box colours assigned depending on the confidence of core position and order; green for high, yellow for medium and red for low confidence.

The PilotSTRATEGY project has received funding from the European Union's Horizon 2020 research and innovation programme under grant agreement No. 101022664



@PilotSTRATEGY  
 www.pilotstrategy.eu  
 Page 43



**Core data**

Core #1: 413.00-422.00m, recovered 7.70m (86%)

Core #2: 511.20-520.20m, recovered 9.00m (100%)

Core #3: 1036.00-1040.00m, recovered 5.00m (100%)

Core #4: 1075.30-1080.30m, recovered 5.00m (100%)



**Confidence about the core position/order**

- High** (Green)
- Medium** (Yellow)
  - no labels but signs of matching with vintage data
  - contradicts vintage data and other boxes
- Low** (Red)
  - no labels
  - severe reposition of core in box
  - Complete mismatch with vintage data
  - Missing core/box issues

Core photos from Neapolis-2 well in MHB. Notice that cores #3 and #4 have been taken from the basement section. Box colours assigned depending on the confidence of core position and order; green for high, yellow for medium and red for low confidence.

The PilotSTRATEGY project has received funding from the European Union’s Horizon 2020 research and innovation programme under grant agreement No. 101022664

